LargeBRAT: A Decomposition Scheme for Large Backward Reach-Avoid Tubes.

Olalekan Ogunmolu[1], Sylvia Herbert[2].

***Abstract*—Backward reachability analysis verifies a robustness metric that guarantees system safety. However, it is premised on solving implicitly-constructed value functions on spatio-temporal grids to verify a robustness metric that guarantees system safety – up to a specified time bound. However, as state dimensions increase, time-space discretization methods become impractical owing to their exponential complexity. Approximation schemes in global value function space fail to preserve the robustness guarantees of basic backward reachability theory. We present an iterative decomposition scheme that incrementally truncates a high-dimensional value function to the minimum low-rank tensor necessary for computing reachable sets, tubes and reach-avoid with guarantee to a local saddle-point extrema. This paper presents an initial evaluation of our proposal on the backward reachable sets and a classical time-optimal bang-bang control time-to-reach the origin problem.**

I. INTRODUCTION.

Designed cyberphysical systems (CPS) are a complex interconnection of control systems, sensors, and their software whose communication protocols have created complex entanglements with interactions that are difficult to analyze. CPS are traditionally engineered to sense and interact with the physical world "smartly". Modern cyberphysical systems may include modern manufacturing assembly lines where humans and machines jointly work to deliver products to a supply chain controlled by computer software resources, personalized interoperable medical devices, autonomous cars on a highway, (almost unmanned) long-hauled passenger flights, or general logistics inter alia.

The "physical" and "cyber" couplings of such systems is critical in modern CPS infrastructure: generating control laws – where dynamics may be complex; planning and executing in real-time collision avoidance schemes in uneven terrains, or sensing efficiently in the presence of multiple agents – all require deep integration and the actions of system components must be planned meticulously. Therefore, the safety analysis of combined CPS systems in the presence of sensing, control, and learning becomes timely and crucial. Differential optimal control theory and games offer a powerful paradigm for resolving the safety of multiple agents interacting over a shared space. Both problems rely on a resolution of the Hamilton-Jacobi-Bellman (HJB) or the Hamilton-Jacobi-Isaacs (HJI) equation in order to solve the control problem. As HJ-type equations have no classical solution for almost all *practical* problems, stable numerical and computational methods need to be brought to bear in order to produce solutions with (approximately) optimal guarantees.

With essentially non-oscillating (ENO) [1] Lax-Friedrichs [2] schemes applied to numerically resolve HJ Hamiltonians [3], we can now obtain unique (viscosity) solutions to HJ-type equations with high accuracy and precision *on a mesh*. Employing meshes for resolving inviscid Euler equations whose solutions are the derivatives of HJ equations, these methods scale exponentially with state dimensions, making them ineffective for complex systems – a direct consequence of *curse of dimensionality* [4]. Truncated power series methods [5]–[8] are successive approximations of HJ value functions; however, these limit the stability region of the resulting approximate controller, and require a careful tuning of the approximate controller such that it has a direct effect on the original optimal control problem. In addition, stability is not easily guaranteed for series approximated HJ value functions where it is generally assumed that the highest-ordered terms in the series truncation dominate neglected higher-order terms.

Therefore in subject matter and emphasis, this paper reflects the influences described in the foregoing. As a result, we focus on computational techniques because almost all *practical* problems cannot be analytically resolved. To analyze safety, we cast our problem formulation within the framework of *Cauchy-type* HJ equations [9], and we resolve the scalable safety problem by solving the unconstrained continuous-time terminal value optimal control problem[1] with Bolza objective functions.

In this sentiment, new computational techniques are introduced including (i) iterative proper orthogonal decomposition of TO-DO: large value functions; (ii) finite difference approximation schemes with error estimates (essentially, an extension of [11] on reduced Hilbertian spaces); and (iii) analytic saddle solutions to approximated HJI value functions. All of these are employed to synthesize approximately optimal control laws (essentially, saddle-point solutions) TO-DO: with stability guarantees for resolving the terminal value in the viscosity solutions to HJI value functions.

In order to analyze the safety of emerging CPS systems given the computational and memory drawbacks of level sets methods, it is the opinion of the authors that

- easily implementable approximation schemes with stability guarantees;

[1] Microsoft Research, 300 Lafayette Street, New York, NY10012, USA. [2]Department of Mechanical and Aerospace Engineering, UC San Diego, La Jolla, CA, USA. lekanmolu@microsoft.com, sherbert@eng.ucsd.edu.

[1]This is done within the framework of Mitchell's *robustly controlled backward reachable tubes* [10].

- stability in well-defined regions of the state space where approximation is guaranteed to work;
- and low run-time computation and memory requirements that address the jugular of the curse of dimensionality; whilst
- providing bounds on the error in the approximation,

are the best means for tackling this problem.

The rest of this paper is organized as follows: we introduce common notations and definitions in § II; § III describes the concepts and topics we will build upon in describing our proposal in § IV; we present results and insights from experiments in § V. We conclude the paper in § VII. This work is the first to systematically provide a rational incremental decomposition scheme that provides approximation guarantees on regions of the state space where approximate HJ control laws are valid as well as provide a rational analysis for high-dimensional verification of nonlinear systems with guarantees.

II. Notations and Definitions.

Throughout this article, time variables e.g. t, t_0, τ, T will always be real numbers. We let $t_0 \leq t \leq t_f$ denote fixed, ordered values of t. Vectors will be denoted by small boldface letters such as $\mathbf{e}, \mathbf{u}, \mathbf{v}$ e.t.c. An n-dimensional vector will be the set $\{x_1, x_2, \ldots, x_n\}$. Unless otherwise noted, vector elements will be column-wise stacked. When we refer to a row-vector, we shall introduce the transpose as a superscript operator i.e. $\boldsymbol{x}^T$. Matrices and tensors will respectively be denoted by bold-math upper case Latin and double stroke font letters e.g. $\mathbf{T}, \mathbf{S}$ (resp. $\mathbb{T}$, $\mathbb{S}$). We designate uppercase letters I, N, R for tensor sizes (the total number of elements encompassed along a dimension of a tensor), and lowercase letters i, n, r for corresponding tensor indices. Exceptions: the unit matrix is I or I, and i, j, k are indices. We adopt zero-indexing for matrix and tensor operations throughout such that if index i corresponds to size I, we write $i = 0, 1, \cdots, I-1$. Lastly, for a tensor with N modes, we denote by $[N]$ the set $\{0, 1, \cdots, N-1\}$.

A. Vectors, Matrices, and Tensors.

1) Vectors: The norm $\|\mathbf{X}\|$ of a matrix $\mathbf{X}$ is sup $\|\mathbf{X}\|$ over $\|\mathbf{X}\| = 1$. We define the *direction cosines* of the orthonormal basis $\{\mathbf{e}_i'\}$ oriented with respect to $\{\mathbf{e}_j\}$ as $\mathbf{Q}_{ij} = \mathbf{e}_i' \cdot \mathbf{e}_j$. so that by orthonormality and by $\mathbf{e}_i' = \mathbf{Q}_{ik}\mathbf{e}_k \, \forall i = (1, 2, 3)$, we have $\delta_{ij} = \mathbf{e}_i' \cdot \mathbf{e}_j' = \mathbf{Q}_{ik}\,\mathbf{e}_k \cdot \mathbf{e}_j' = \mathbf{Q}_{ik}\mathbf{Q}_{jk}$, where δ_{ij} is the Krönecker delta symbol. The *triple scalar product* $(\mathbf{u} \wedge \mathbf{v}) \cdot \mathbf{w}$ is $(\mathcal{E}_{ijp} u_i v_j \mathbf{e}_p) \cdot (w_k \mathbf{e}_k) = \mathcal{E}_{ijk} u_i v_j w_k$, where $\mathcal{E}_{ijk}$ is the *alternating symbol*. For two vectors $\mathbf{u}$ and $\mathbf{v}$ moving between bases $\{\mathbf{e}_i\}$ and $\{\mathbf{e}_i'\}$, their components' product $u_i v_j$ transform according to the tensor product[2], $(\mathbf{u} \otimes \mathbf{v})_{ij} = u_i' v_j' = \mathbf{Q}_{ip}\mathbf{Q}_{jq} u_p v_q$. Thus, $I = \delta_{ij}\mathbf{e}_i \otimes \mathbf{e}_j := \mathbf{e}_i \otimes \mathbf{e}_j$ for an arbitrary orthonormal basis $\{\mathbf{e}_i\}$.

2) Tensor Algebra: We refer to the *mode-n unfolding* (or *matricization*) of a tensor, $\mathbb{T}$, as the rearrangement of its N elements into a matrix, $\mathbb{T}_n \in \mathbb{R}^{I_n \times \Pi_{k \neq n}^{n-1} I_k}$ where $n \in \{0, 1, \cdots, N-1\}$. The *multilinear rank* of $\mathbb{T} \in \mathbb{R}^{I_0 \times I_1 \cdots \times I_{N-1}}$ is an N-tuple with elements that correspond to the rank of the mode-n vector space i.e., $(R_0, R_1, \cdots, R_{N-1})$. The *Frobenius inner product* induced on the tensor product space $\mathbb{T}_1 \otimes \mathbb{T}_2 \in \mathbb{R}^{I_0 \times I_1 \times I_{n-1} \cdots \times I_{N-1}}$ is

$$\begin{aligned} \langle \mathbb{T}_1, \mathbb{T}_2 \rangle_F &= \text{trace}\left(\mathbb{T}_{2_{(n)}}^T, \mathbb{T}_{1_{(n)}}\right) \\ &= \text{trace}\left(\mathbb{T}_{1_{(n)}}^T, \mathbb{T}_{2_{(n)}}\right) \\ &= \langle \mathbb{T}_2, \mathbb{T}_1 \rangle_F. \end{aligned} \tag{1}$$

By the *norm of a tensor* with dimension N, we shall mean the square root of the sum of squares of all its elements. This is equivalent to the Frobenius norm along any n-mode unfolding, $\mathbb{T}_{(n)}$, of tensor $\mathbb{T}$. Thus,

$$\|\mathbb{T}\|_F^2 := \langle \mathbb{T}, \mathbb{T} \rangle_F = \|\mathbb{T}_{(n)}\|_F^2 \tag{2}$$

for any n-mode unfolding of the tensor. We may otherwise refer to $\|\cdot\|_F$ as the Hilbert-Schmidt norm.

Following the convention delineated in Table **??**, we define the product of tensor $\mathbb{T}$ (of size $I_0 \times I_1 \times I_{n-1} \cdots \times I_{N-1}$) and a matrix $\mathbf{U}$ (of size $J \times I_n$) as

$$\mathbb{P} = \mathbb{T} \otimes_n \mathbf{U} \implies \mathbb{P}_{(n)} = \mathbf{U}\mathbb{T}_{(n)}. \tag{3}$$

For different modes, the ordering of the modes is not consequential so that

$$\mathbb{T} \otimes_n \mathbf{U} \otimes_m \mathbf{V} = \mathbb{T} \otimes_m \mathbf{V} \otimes_n \mathbf{U} \quad \forall\, m \neq n. \tag{4}$$

However, in the same mode, order matters so that $\mathbb{T} \otimes_n \mathbf{U} \otimes_n \mathbf{V} = \mathbb{T} \otimes_n \mathbf{V} \otimes_n \mathbf{U}$. The *multilinear orthogonal projection* from a tensor space with dimension $I_0 \times \cdots I_{n-1} \times I_n \times I_{n+1} \cdots \times I_{N-1}$ onto the subspace $I_0 \times \cdots I_{n-1} \times U_n \times I_{n+1} \cdots \times I_{N-1}$ is the orthogonal projection along mode n given by

$$\pi_n \mathbb{T} := \mathbb{T} \otimes_n \left(\mathbf{I} - \mathbf{U}_n \mathbf{U}_n^T\right). \tag{5}$$

The rest of the notations we use for tensor operations in this article are described in Table **??**. We refer readers to [12], [13] for a detailed description of other tensor algebraic notations and multilinear operations.

B. Sets, Controls, and Games.

The set S of all $\boldsymbol{x}$ such that $\boldsymbol{x}$ belongs to the real numbers $\mathbb{R}$, and that $\boldsymbol{x}$ is positive will be written as $S = \{\boldsymbol{x} \,|\, \boldsymbol{x} \in \mathbb{R}, \boldsymbol{x} > 0\}$. We define Ω as the open set in $\mathbb{R}^n$. To avoid the cumbersome phrase "the state $\boldsymbol{x}$ at time t", we will associate the pair $(\boldsymbol{x}, t)$ with the *phase* of the system for a state $\boldsymbol{x}$ at time t. Furthermore, we associate the Cartesian product of Ω and the space $T = \mathbb{R}^1$ of all time values as the *phase space* of $\Omega \times T$. The interior of Ω is denoted by int Ω; whilst the closure of Ω is denoted $\bar{\Omega}$. We denote by $\delta\Omega\,(:= \bar{\Omega} \backslash \text{int } \Omega)$ the boundary of the set Ω.

Unless otherwise stated, vectors $\boldsymbol{u}(t)$ and $\boldsymbol{v}(t)$ are reserved for admissible control (resp. disturbance) at time t. We say $\boldsymbol{u}(t)$ (resp. $\boldsymbol{v}(t)$) is piecewise continuous in t, if for each t, $\boldsymbol{u} \in \mathcal{U}$ (resp. $\boldsymbol{v} \in \mathcal{V}$), $\mathcal{U}$(resp. $\mathcal{V}$) is a Lebesgue measurable and compact set.

At all times, any of $\boldsymbol{u}$ or $\boldsymbol{v}$ will be under the influence of a *player* such that the motion of a state $\boldsymbol{x}$ will be influenced by

[2] Or the dyadic product.

Tensor Operations

Notation	Description
$\mathbb{T}_n$	n-mode unfolding of $\mathbb{T}$.
$\mathbf{G} = \mathbb{T}_n \mathbb{T}_n^T$	Gram matrix.
$[N] = \{0, 1, \cdots, N-1\}$	Total number of modes in $\mathbb{T}$.
$\|\mathbb{T}\|_F$	The Hilbert-Schmidt norm of $\mathbb{T}$.
$\mathbb{T} \otimes_n \mathbf{U}$	n-mode product of $\mathbb{T}$ with matrix $\mathbf{U}$.
$\mathbb{T} \hat{\otimes}_n \mathbf{v}$	n-mode product of $\mathbb{T}$ with vector $\mathbf{v}$.
$\mathbb{T} \circledast \mathbf{S}$	Kronecker product of $\mathbb{T}$ with matrix $\mathbf{S}$.
$\mathbb{T} \odot \mathbf{S}$	Khatri-Rao product of $\mathbb{T}$ with matrix $\mathbf{S}$.

Differential Optimal Control and Games

a.e.	Almost everywhere.
$\boldsymbol{\xi}$	System trajectory.
$\boldsymbol{P}$, $\boldsymbol{E}$	Pursuer and Evader respectively.
$\langle \cdot, \cdot \rangle$	The dot product operator.
$\boldsymbol{V}(t, \boldsymbol{x})$	Value function of the differential game.
$\boldsymbol{V}_{\boldsymbol{x}}(t, \boldsymbol{x})$, $\boldsymbol{V}_t(t, \boldsymbol{x})$	Spatial derivative (resp. time derivative) of $\boldsymbol{V}$.
$\boldsymbol{V}^-(t, \boldsymbol{x})$, $\boldsymbol{V}^+(t, \boldsymbol{x})$	Lower and upper values of the differential game.
$\boldsymbol{H}^-(t; \cdot)$, $\boldsymbol{H}^+(t; \cdot)$	A game's lower and upper Hamiltonians.
$\bar{\mathcal{U}}$, $\bar{\mathcal{V}}$	Controls set for $\boldsymbol{P}$ and $\boldsymbol{E}$ respectively.
$\mathcal{A}(t)$, $\mathcal{B}(t)$	Strategies set for $\boldsymbol{P}$ and $\boldsymbol{E}$, starting at t.
$\mathcal{F}(t, \boldsymbol{x}; \cdot)$	A separable Hilbert-space where $\boldsymbol{x}$ is defined.
$\mathcal{F}^\star(t, \boldsymbol{x}; \cdot)$	Dual of the separable Hilbert-space, $\mathcal{F}(\cdot)$.
$\mathcal{L}_0(\tau)$	A differential game's target set.
$\mathcal{L}([t, 0], \tau)$	A differential game's backward reachable set.

the coercion of that player. Our theater of operations is that of conflicting objectives between players – so that the problem at hand assumes that of a *game*. And by a game, we do not necessarily refer to a single game, but rather a collection of games. Each player in a game will constitute either a pursuer ($\boldsymbol{P}$) or an evader ($\boldsymbol{E}$).

III. Background and Preliminaries.

A. Dynamic Programming and Two-Person Games.

The formal relationships between the dynamic programming (DP) optimality condition for the *value* in differential two-person zero-sum games, and the solutions to PDEs that solve "min-max" or "max-min" type nonlinearity (the Isaacs' equation) was presented in [14]. Essentially, Isaacs' claim was that if the *value* functions are smooth enough, then they solve certain first-order partial differential equations (PDE) problems with "max-min" or "min-max"-type nonlinearity. However, the DP value functions are seldom regular enough to admit a solution in the classical sense. "Weaker" solutions on the other hand [2], [3], [11], [15], [16] provide generalized "viscosity" solutions to HJ PDEs under relaxed regularity conditions; these viscosity solutions are not necessarily differentiable anywhere in the state space, and the only regularity prerequisite in the definition is continuity [9]. However, wherever they are differentiable, they satisfy the upper and lower values of HJ PDEs in a classical sense. Thus, they lend themselves well to many real-world problems existing at the interface of discrete, continuous, and hybrid systems [10], [16]–[19]. Matter-of-factly, viscosity Solutions to *Cauchy-type* HJ Equations admit usefulness in backward reachability analysis [19]. In scope and focus, this is the bulwark upon which we build our formulation in this paper.

For a state $\boldsymbol{x} \in \Omega$ and a fixed time t: $0 \leq t < T$, suppose that the set of all controls for players $\boldsymbol{P}$ and $\boldsymbol{E}$ are respectively

$$\bar{\mathcal{U}} \equiv \{\boldsymbol{u} : [t, T] \to \mathcal{U} | \boldsymbol{u} \text{ measurable}, \mathcal{U} \in \mathbb{R}^m\}, \tag{6}$$

$$\bar{\mathcal{V}} \equiv \{\boldsymbol{v} : [t, T] \to \mathcal{V} | \boldsymbol{v} \text{ measurable}, \mathcal{V} \subset \mathbb{R}^p\}. \tag{7}$$

We are concerned with the differential equation,

$$\dot{\boldsymbol{x}}(\tau) = f(\tau, \boldsymbol{x}(\tau), \boldsymbol{u}(\tau), \boldsymbol{v}(\tau)) \quad T \leq \tau \leq t \tag{8a}$$

$$\boldsymbol{x}(t) = \boldsymbol{x}, \tag{8b}$$

where $f(\tau, \cdot, \cdot, \cdot)$ and $\boldsymbol{x}(\cdot)$ are bounded and Lipschitz continuous. This bounded Lipschitz continuity property assures uniqueness of the system response $\boldsymbol{x}(\cdot)$ to controls $\boldsymbol{u}(\cdot)$ and $\boldsymbol{v}(\cdot)$ [16]. Associated with (8) is the payoff functional

$$\begin{aligned} \boldsymbol{P}(\boldsymbol{u}, \boldsymbol{v}) &= \boldsymbol{P}(t; \boldsymbol{x}, \boldsymbol{u}(\cdot), \boldsymbol{v}(\cdot)) \\ &= \int_t^T l(\tau, \boldsymbol{x}(\tau), \boldsymbol{u}(\tau), \boldsymbol{v}(\tau)) d\tau + g(\boldsymbol{x}(T)), \end{aligned} \tag{9}$$

where $g(\cdot) : \mathbb{R}^n \to \mathbb{R}$ satisfies

$$|g(\boldsymbol{x})| \leq k_1 \tag{10a}$$

$$|g(\boldsymbol{x}) - g(\hat{\boldsymbol{x}}) \,| \leq k_1 |\boldsymbol{x} - \hat{\boldsymbol{x}} \,| \tag{10b}$$

and $l : [0, T] \times \mathbb{R}^n \times \mathcal{U} \times \mathcal{V} \to \mathbb{R}$ is bounded and uniformly continuous, with

$$| \, l(t; \boldsymbol{x}, \boldsymbol{u}, \boldsymbol{v}) \, | \leq k_2 \tag{11a}$$

$$| \, l(t; \boldsymbol{x}, \boldsymbol{u}, \boldsymbol{v}) - l(t; \hat{\boldsymbol{x}}, \boldsymbol{u}, \boldsymbol{v}) \, | \leq k_2 \, | \, \boldsymbol{x} - \hat{\boldsymbol{x}} \, | \tag{11b}$$

for constants k_1, k_2 and all $0 \leq t \leq T$, $\hat{\boldsymbol{x}}, \boldsymbol{x} \in \mathbb{R}^n$, $\boldsymbol{u} \in \mathcal{U}$ and $\boldsymbol{v} \in \mathcal{V}$. We call T is the *terminal time* (it may be infinity!) and the integral, when it does not depend on the control laws, is the *performance index*. The evader's goal is to maximize the payoff (9) and pursuer's goal is to minimize it.

B. Upper and Lower Values of the Differential Game.

Suppose that the pursuer's mapping strategy (starting at t) is $\beta : \bar{\mathcal{U}}(t) \to \bar{\mathcal{V}}(t)$ provided for each $t \leq \tau \leq T$ and $\boldsymbol{u}, \hat{\boldsymbol{u}} \in \bar{\mathcal{U}}(t)$; then $\boldsymbol{u}(\bar{t}) = \hat{\boldsymbol{u}}(\bar{t})$ a.e. on $t \leq \bar{t} \leq \tau$ implies $\beta[\boldsymbol{u}](\bar{t}) = \beta[\hat{\boldsymbol{u}}](\bar{t})$ a.e. on $t \leq \bar{t} \leq \tau$. The differential game's lower value for a solution $\boldsymbol{x}(t)$ that solves (8) for $\boldsymbol{u}(t)$ and $\boldsymbol{v}(t) = \beta[\boldsymbol{u}](\cdot)$ is

$$\begin{aligned} \boldsymbol{V}^-(\boldsymbol{x}, t) &= \inf_{\beta \in \mathcal{B}(t)} \sup_{\boldsymbol{u} \in \bar{\mathcal{U}}(t)} \boldsymbol{P}(\boldsymbol{u}, \beta[\boldsymbol{u}]) \\ &= \inf_{\beta \in \mathcal{B}(t)} \sup_{\boldsymbol{u} \in \bar{\mathcal{U}}(t)} \int_t^T l(\tau, \boldsymbol{x}(\tau), \boldsymbol{u}(\tau), \beta[\boldsymbol{u}](\tau)) d\tau + g\left(\boldsymbol{x}(T)\right). \end{aligned} \tag{12}$$

Similarly, suppose that the evader's mapping strategy (starting at t) is $\alpha : \bar{\mathcal{V}}(t) \to \bar{\mathcal{U}}(t)$ provided for each $t \leq \tau \leq T$ and $\boldsymbol{v}, \hat{\boldsymbol{v}} \in \bar{\mathcal{V}}(t)$; then $\boldsymbol{v}(\bar{t}) = \hat{\boldsymbol{v}}(\bar{t})$ a.e. on $t \leq \bar{t} \leq \tau$ implies $\alpha[\boldsymbol{v}](\bar{t}) = \alpha[\hat{\boldsymbol{v}}](\bar{t})$ a.e. on $t \leq \bar{t} \leq \tau$. The differential

game's upper value for a solution $\boldsymbol{x}(t)$ that solves (8) for $\boldsymbol{u}(t) = \alpha[\boldsymbol{v}](\cdot)$ and $\boldsymbol{v}(t)$ is

$$\begin{aligned}\boldsymbol{V}^{+}(\boldsymbol{x},t) &= \sup_{\alpha\in\mathcal{A}(t)}\inf_{\boldsymbol{v}\in\mathcal{V}(t)}\boldsymbol{P}(\alpha[\boldsymbol{v}],\boldsymbol{v}) \\ &= \sup_{\alpha\in\mathcal{A}(t)}\inf_{v\in\mathcal{V}(t)}\int_{t}^{T} l(\tau,\boldsymbol{x}(\tau),\alpha[\boldsymbol{v}](\tau),\boldsymbol{v}(\tau))d\tau + g\left(\boldsymbol{x}(T)\right).\end{aligned} \tag{13}$$

These non-local PDEs i.e. (12) and (13) are hardly smooth throughout the state space so that they lack classical solutions even for smooth Hamiltonian and boundary conditions. However, these two values are "viscosity" (generalized) solutions [9], [15] of the associated HJ-Isaacs (HJI) PDE, i.e. solutions which are *locally Lipschitz* in $\Omega\times[0,T]$, and with at most first-order partial derivatives in the Hamiltonian. In what follows, we introduce the notion of viscosity solutions to the HJI value functionals in (13), and (12).

C. Viscosity Solution of HJ-Isaac's Equations.

For any optimal control problem a value function is constructed based on the optimal cost (or payoff) of any input phase $(\boldsymbol{x},T)$. In reachability analysis, typically this is defined using a terminal cost function $g(\cdot):\mathbb{R}^n\to\mathbb{R}$ that satisfies

$$|g(\boldsymbol{x})| \le k \tag{14a}$$
$$|g(\boldsymbol{x}) - g(\hat{\boldsymbol{x}})\,| \le k|\boldsymbol{x}-\hat{\boldsymbol{x}}\,| \tag{14b}$$

for constant k and all $T\le t\le 0$, $\hat{\boldsymbol{x}}$, $\boldsymbol{x}\in\mathbb{R}^n$, $\boldsymbol{u}\in\mathcal{U}$ and $\boldsymbol{v}\in\mathcal{V}$. The zero sublevel set of $g(\boldsymbol{x})$ i.e.

$$\mathcal{L}_0 = \{\boldsymbol{x}\in\bar{\Omega}\,|\,g(\boldsymbol{x})\le 0\}, \tag{15}$$

Lemma 1. *The lower value $\boldsymbol{V}^{-}$ in (12) is the viscosity solution to the lower Isaac's equation*

$$\frac{\partial \boldsymbol{V}^{-}}{\partial t} + \boldsymbol{H}^{-}(t;\boldsymbol{x},\boldsymbol{u},\boldsymbol{v},\boldsymbol{V}^{-}_{\boldsymbol{x}}) = 0,\ t\in[0,T]\ \boldsymbol{x}\in\mathbb{R}^n \tag{16a}$$
$$\boldsymbol{V}^{-}(\boldsymbol{x},T) = g(x(T)),\quad \boldsymbol{x}\in\mathbb{R}^m \tag{16b}$$

with lower Hamiltonian,

$$\boldsymbol{H}^{-}(t;\boldsymbol{x},\boldsymbol{u},\boldsymbol{v},p) = \max_{u\in\mathcal{U}}\min_{v\in\mathcal{V}}\langle f(t;\boldsymbol{x},\boldsymbol{u},\boldsymbol{v}),p\rangle. \tag{17}$$

where p, the co-state, is the spatial derivative of $\boldsymbol{V}^{-}$ w.r.t $\boldsymbol{x}$.

Lemma 2. *The upper value $\boldsymbol{V}^{+}$ in (13) is the viscosity solution of the upper Isaac's equation*

$$\frac{\partial \boldsymbol{V}^{+}}{\partial t} + \boldsymbol{H}^{+}(t;\boldsymbol{x},\boldsymbol{u},\boldsymbol{v},\boldsymbol{V}^{+}_{\boldsymbol{x}}) = 0,\ t\in[0,T]\,,\ \boldsymbol{x}\in\mathbb{R}^n \tag{18a}$$
$$\boldsymbol{V}^{+}(\boldsymbol{x},T) = g(\boldsymbol{x}(T)),\quad \boldsymbol{x}\in\mathbb{R}^n \tag{18b}$$

with upper Hamiltonian,

$$\boldsymbol{H}^{+}(t;\boldsymbol{x},\boldsymbol{u},\boldsymbol{v},p) = \min_{\boldsymbol{v}\in\mathcal{V}}\max_{\boldsymbol{u}\in\mathcal{U}}\langle f(t;\boldsymbol{x},\boldsymbol{u},\boldsymbol{v}),p\rangle, \tag{19}$$

with p being appropriately defined.

Corollary 1. *(i) $\boldsymbol{V}^{-}\le\boldsymbol{V}^{+}$ over $(t\in[0,T]\ \boldsymbol{x}\in\mathbb{R}^n)$ (ii) if for all $t\in[0,T]\,,(\boldsymbol{x},p)\in\mathbb{R}^n$, the minimax condition is satisfied i.e. $\boldsymbol{H}^{+}(t;\boldsymbol{x},\boldsymbol{u},\boldsymbol{v},p) = \boldsymbol{H}^{-}(t;\boldsymbol{x},\boldsymbol{u},\boldsymbol{v},p)$, then $\boldsymbol{V}^{-}\equiv\boldsymbol{V}^{+}$.*

D. Reachability for Systems Verification.

Reachability analysis is one of many verification methods that allows us to reason about (control-affine) dynamical systems. The verification problem may consist in finding a *set of reachable states* that lie along the trajectory of the solution to a first order nonlinear partial differential equation that originates from some initial state $\boldsymbol{x}_0 = \boldsymbol{x}(0)$ up to a specified time bound, $t = t_f$. *From a set of initial and unsafe state sets, and a time bound, the time-bounded safety verification problem is to determine if there is an initial state and a time within the bound that the solution to the PDE enters the unsafe set.*

Reachability could be analyzed in a

- *forward* sense, whereupon system trajectories are examined to determine if they enter certain states from an *initial set*;
- *backward* sense, whereupon system trajectories are examined to determine if they enter certain *target sets*;
- *reach set* sense, in which they are examined to see if states reach a set at a *particular time*; or
- *reach tube* sense, in which they are evaluated that they reach a set at a point *during a time interval*.

Backward reachability consists in avoiding an unsafe set of states under the worst-possible disturbance at all times; relying on nonanticipative control strategies, [19]'s construction does not necessarily use a state feedback control law during games and the worst-possible disturbance assumption is not formally inculcated in the backward reachability analyses used. In a sense, it is reasonable to ignore nonlinear $\mathcal{H}^2$ or $\mathcal{H}^\infty$ analyses for Dubins vehicle [20] dynamics with constant inputs that only vary in sign for either player [21] since the worst possible disturbance is known ahead of the game. In other problem domains, this is not sufficient, TO-DO: and in our analyses we provide an $\mathcal{H}^\infty$ scheme [22]'s in constructing an appropriate *worst-possible* disturbance that guarantees robustness in continuous control applications.

Backward reachable sets (BRS) or tubes (BRTs) are popularly analyzed an a game of two vehicles with non-stochastic dynamics [21]. Such BRTs possess discontinuity at crossover points (which exist at edges) on the surface of the tube, and may be non-convex. Therefore, treating the end-point constraints under these discontinuity characterizations need careful consideration and analysis when switching control laws if the underlying P.D.E does not have continuous partial derivatives (we discuss this further in section IV).

1) Insufficiency of Global Mesh-based Methods: Consider a reachability problem defined in a space of dimension $D = 12$ based on the non-incremental time-space discretization of each space coordinate. For $N = 100$ nodes, the total nodes required is 10^{120} on the volumetric grid[3]. The curse of dimensionality [4] greatly incapacitates current uniform grid discretization methods for guaranteeing the robustness of backward reachable sets (BRS) and tubes (BRTs) [19] of complex systems.

Recent works have started exploring scaling up the Cauchy-type HJ problem for guaranteeing safety of higher-dimensional

[3]Whereas, there are only 10^{97} baryons in the observable universe (excluding dark matter)!

physical systems: the authors of [23] provide local updates to BRS in unknown static environments with obstacles that may be unknown *a priori* to the agent; using standard meshing techniques for time-space uniform discretization over the entire physical space, and only updating points traversed locally, a safe navigation problem was solved in an environment assumed to be static. This makes it non-amenable to *a priori* unknown *dynamic* environments where the optimal value to the min-max HJ problem may need to be adaptively updated based on changing dynamics.

In [24], the grid was naively refined along the temporal dimension, leveraging local decomposition schemes together with warm-starting optimization of the value function from previous solutions in order to accelerate learning for safety under the assumption that the system is either completely decoupled, or coupled over so-called "self-contained subsystems". While the empirical results of [25] demonstrate the feasibility of optimizing for the optimal value function in backward reachability analysis for up to ten dimensions for a system of Dubins vehicles, there are no guarantees that are provided. An analysis exists for a 12 dimensional systems [26] with up to a billion data points in the state space, that generates robustly optimal trajectories. However, this is restricted to linear systems. Other associated techniques scale reachability with function approximators [27], [28] in a reinforcement learning framework; again these methods lose the hard safety guarantees owing to the approximation in value function space.

In these sentiments, we seek to answer the following questions for high-dimensional systems:

- What role does sparsity play in the representation of BRTs and BRS's for high-order systems?
- Can we provide rational decomposition schemes that preserve the numerical stability of monotone Lax-Friedrichs and essentially non-oscillatory [1] gradient methods to the HJ values and Hamiltonians?
- How scalable are self-contained subsystems partitioning of state spaces [29] to complex systems with possibly high dimensional state spaces?
- With projection to reduced order systems, can we relax the strong assumptions made in local decomposition [29], [30] e.g. about the dynamics of the global system consisting of separable subsystems?

We briefly answer the first question. As long as value functions are implicitly defined as signed distance value functions on a grid, there is no possibility of exploiting sparsity for high-dimensional value functions. This is because these value functions are constructed with signed distance functions with respect to an interface on the grid [31, Chapter 2]. The value function is positive within the interface and negative outside the interface. Therefore, the representation of such values are completely dense. Unless we can find methods to sparsely represent the value function on a grid, exploiting sparsity of the value function is hopeless. In the sections that follow, we seek to answer the other questions posed above.

2) Reachability from Differential Games Optimal Control: For any admissible control-disturbance pair $(\boldsymbol{u}(\cdot), \boldsymbol{v}(\cdot))$ and initial phase $(\boldsymbol{x}_0, t_0)$, Crandall [9] and Evan's [3] claim is that there exists a unique function

$$\boldsymbol{\xi}(t) = \boldsymbol{\xi}(t; t_0, \boldsymbol{x}_0, \boldsymbol{u}(\cdot), \boldsymbol{v}(\cdot)) \tag{20}$$

that satisfies (8) a.e. with the property that

$$\boldsymbol{\xi}(t_0) = \boldsymbol{\xi}(t_0; t_0, \boldsymbol{x}_0, \boldsymbol{u}(\cdot), \boldsymbol{v}(\cdot)) = \boldsymbol{x}_0. \tag{21}$$

Read (20): the motion of (8) passing through phase $(\boldsymbol{x}_0, t_0)$ under the action of control $\boldsymbol{u}$, and disturbance $\boldsymbol{v}$, and observed at a time t afterwards. One way to design a system verification problem is compute the reachable set of states that lie along the trajectory (20) such that we evade the unsafe sets up to a time e.g. t_f within a given time bound e.g. $[t_0, t_f]$. In this regard, we discard the *cost-to-go*, $l(t; \boldsymbol{x}(\tau), \boldsymbol{u}(\tau), \boldsymbol{v}(\tau))$ in (9), (12), or (13) and certify safety as resolving the terminal value, $g(\boldsymbol{x}(T))$.

In backward reachability analysis, the lower value of the differential game i.e. (12) is used in constructing an analysis of the backward reachable set (or tube). Therefore, we can cast a target set as the time-resolved terminal value $\boldsymbol{V}^-(\boldsymbol{x}, T) = g(\boldsymbol{x}(T))$ so that given a time bound, and an unsafe set of states, the time-bounded safety verification problem consists in certifying that there is no phase within the target set (22) such that the solution to (8) enters the unsafe set. Following the backward reachability formulation of [19], we say the zero sublevel set of $g(\cdot)$ in (16) i.e.

$$\mathcal{L}_0 = \{\boldsymbol{x} \in \bar{\Omega} \,|\, g(\boldsymbol{x}) \leq 0\}, \tag{22}$$

is the *target set* in the phase space $\Omega \times \mathbb{R}$ for a backward reachability problem (proof in [19]). This target set can represent the failure set, regions of danger, or obstacles to be avoided etc in the state space. Note that the target set, $\mathcal{L}_0$, is a closed subset of $\mathbb{R}^n$ and is in the closure of Ω. And the *robustly controlled backward reachable tube* for $\tau \in [-T, 0]$[4] is the closure of the open set

$$\begin{aligned}\mathcal{L}([\tau, 0], \mathcal{L}_0) = \{\boldsymbol{x} \in \Omega \,|\, \exists\, \beta \in \bar{\mathcal{V}}(t)\, \forall\, \boldsymbol{u} \in \mathcal{U}(t), \exists\, \bar{t} \in [-T, 0], \\ \boldsymbol{\xi}(\bar{t}) \in \mathcal{L}_0\},\ \bar{t} \in [-T, 0]\,.\end{aligned} \tag{23}$$

Read: the set of states from which the strategies of $\boldsymbol{P}$, and for all controls of $\boldsymbol{E}$ imply that we reach the target set within the interval $[T, 0]$. More specifically, following Lemma 2 of [19], the states in the reachable set admit the following properties w.r.t the value function $\boldsymbol{V}$

$$\boldsymbol{x} \in \mathcal{L}_0 \implies \boldsymbol{V}^-(\boldsymbol{x}, t) \leq 0 \tag{24a}$$

$$\boldsymbol{V}^-(\boldsymbol{x}, t) \leq 0 \implies \boldsymbol{x} \in \mathcal{L}_0. \tag{24b}$$

Observe:

- The goal of the pursuer, or $\boldsymbol{P}$, is to drive the system's trajectories into the unsafe set i.e., $\boldsymbol{P}$ has $\boldsymbol{u}$ at will and aims to minimize the termination time of the game (c.f. (22));
- The evader, or $\boldsymbol{E}$, seeks to avoid the unsafe set i.e., $\boldsymbol{E}$ has controls $\boldsymbol{v}$ at will and seeks to maximize the termination time of the game (c.f. (22));
- $\boldsymbol{E}$ has regular controls, $\boldsymbol{u}$, drawn from a Lebesgue measurable set, $\mathcal{U}$ (c.f. (12)).

[4]The (backward) horizon, $-T$ is negative for $T > 0$.

- $\boldsymbol{P}$ possesses *nonanticipative strategies* (c.f. (12)) i.e. $\beta[\boldsymbol{u}](\cdot)$ such that for any of the ordinary controls, $\boldsymbol{u}(\cdot) \in \mathcal{U}$ of $\boldsymbol{E}$, $\boldsymbol{P}$ knows how to optimally respond to $\boldsymbol{E}$'s inputs.

This is a classic reachability problem on the resolution of the infimum-supremum over the *strategies* of $\boldsymbol{P}$ and *controls* of $\boldsymbol{E}$ with the time of capture resolved as an extremum of a cost functional) over a time interval.

TO-DO: We obtain a *pseudo iterative dynamic game* [32], albeit in open-loop settings, where either player infers the current state useful enough for generating closed-loop input control laws. An implicit surface function, $\{\boldsymbol{V}^{-}(\boldsymbol{x},t) : [-T,0]\times\mathcal{X}\to\mathbb{R}, \forall\, t>0\}$ i.e. the terminal value $\boldsymbol{V}^{-}(\boldsymbol{x},t)$, that characterizes the target set $\mathcal{L}_0$ is the viscosity solution to the HJI PDE

$$\frac{\partial \boldsymbol{V}^{-}}{\partial t}(\boldsymbol{x},t) + \min\{0, \boldsymbol{H}^{-}(t;\boldsymbol{x},\boldsymbol{u},\boldsymbol{v},\boldsymbol{V}^{-}_{\boldsymbol{x}})\} = 0 \tag{25a}$$

$$\boldsymbol{V}^{-}(\boldsymbol{x},0) = g(\boldsymbol{x}), \tag{25b}$$

where the vector field $\boldsymbol{V}^{-}_{\boldsymbol{x}}$ is known in terms of the game's terminal conditions so that the overall game is akin to a two-point boundary-value problem. Henceforward, for ease of readability, we will remove the minus superscript on the lower value and Hamiltonian (17).

IV. Decomposition Scheme.

A. Decomposition Rationale.

Multilinear compositions of linear forms are an efficient way of manipulating complex systems. Higher-order tensors, in particular, are increasingly playing crucial roles in the storage, analysis, and use of high-dimensional data. Applications range from deep learning, higher-order statistics, chemometrics, psychometrics to signal processing inter alia. Evidence abounds that linearized nonlinear system dynamics, truncated at a reduced order r-th mode (e.g. in power series expansions [6], [32]–[34]) admit a higher precision and accuracy of the approximation of the underlying nonlinear system since the moments and accumulations of higher-order dynamics are equivalent to the power series expansion coefficients.

In this section, we introduce a multilinear decomposition scheme for decomposing large backward reachable tubes in order to alleviate the exponential complexity of mesh constraints; it is an iterative scheme that generates separable reduced order models (ROM) of the original value function, which are respectively compactly represented on a mesh – making our method amenable to resolving terminal value functions using level sets methods. In [19], Mitchell showed that by giving the pursuer an advantage with a nonanticipative strategy in the two-person game, the reachable set is overapproximated in the Lax-Friedrichs numerical scheme used. In our decomposition scheme, we follow the same non-anticipative strategies for the pursuer on the reduced basis. Hence, our decomposition scheme admits an overapproximation of the reachable set in some sense.

B. Separable Representations of the ROM Cost Functional

Let $\mathcal{S}$ be a measurable multidimensional set, including one of possibly infinite dimensions such as $\{\psi_i\}_{i=0}^{\infty} \in \mathcal{S}$. Furthermore, let the functional space $L^2(\mathcal{S};\mathcal{F})$ be the class of functions $\{\boldsymbol{\phi}_i(\boldsymbol{x})\}_i^{\infty} \in \mathcal{F}$ whose second powers are measurable over the set $\mathcal{S}$ and for which

$$\int_{\mathcal{S}} \psi(t)\, \|\boldsymbol{\phi}(\boldsymbol{x})\|^2\, d\boldsymbol{x} < +\infty. \tag{26}$$

Suppose that for another $\boldsymbol{\phi}'(\boldsymbol{x}) \in \mathcal{F}$, we have

$$\langle \boldsymbol{\phi}(\boldsymbol{x}), \boldsymbol{\phi}'(\boldsymbol{x})\rangle = \int_{\mathcal{S}} \psi(t)\, \left[\boldsymbol{\phi}(\boldsymbol{x})\, \overline{\boldsymbol{\phi}'(\boldsymbol{x})}\right] dt, \tag{27}$$

then $L^2(\mathcal{S};\mathcal{F})$ becomes a Hilbert space, where $\bar{\boldsymbol{\phi}}'(\boldsymbol{x})$ is the complex conjugate of $\boldsymbol{\phi}(\boldsymbol{x})$. The finiteness of $\langle \boldsymbol{\phi}(\boldsymbol{x}), \boldsymbol{\phi}'(\boldsymbol{x})\rangle$ follows from Bunyakovskii's inequality i.e. $|\langle \boldsymbol{\phi}(\boldsymbol{x}), \boldsymbol{\phi}'(\boldsymbol{x})\rangle| \leq \infty$. In addition, the inner product associated with $L^2(\mathcal{S},\mathcal{F})$ induces a norm[5] in $L^2(\mathcal{S};\mathcal{F})$ which is given by

$$\|\boldsymbol{\phi}(\boldsymbol{x})\| = \left[\int_{\mathcal{S}} \psi(t) \|\boldsymbol{\phi}(\boldsymbol{x})\|^2 d\boldsymbol{x}\right]^{\frac{1}{2}}. \tag{28}$$

The space $L^2(\mathcal{S};\mathcal{F})$ is separable so that we can take a denumerable dense set of polynomial expansions in it [35].

C. Decomposition Layout

Following the outline of the denumerable construction of functions $\boldsymbol{\phi}(\boldsymbol{x}) \in L^2(\mathcal{S};\mathcal{F})$ above, we consider separated representations of the value function $\boldsymbol{V}(\boldsymbol{x},t)$ into time functions alone i.e. $\boldsymbol{\psi}(t) \in \mathcal{S}$ and space functions alone i.e. $\boldsymbol{\phi}(\boldsymbol{x}) \in \mathcal{F}$. Let us call this approximation $\boldsymbol{V}(\boldsymbol{x},t;\boldsymbol{\psi})$, and let it possess real values on $L^2(\mathcal{S};\mathcal{F})$.

In this sentiment, $\boldsymbol{V}(\boldsymbol{x},t;\boldsymbol{\psi})$ is the sum of the tensor products of rational coefficients $\{\boldsymbol{\psi}_i\}_{i=0}^{\infty} \in \mathcal{S}$ and polynomial basis functions $\{\boldsymbol{\phi}_i\}_{i=0}^{\infty} \in \mathcal{F}$ that satisfy

$$\boldsymbol{V}(\boldsymbol{x},t) \approx \boldsymbol{V}(\boldsymbol{x},t;\boldsymbol{\psi}) \tag{29a}$$

$$\equiv \sum_{i=0}^{\infty} \boldsymbol{\psi}_i(t)\, \boldsymbol{\phi}_i(\boldsymbol{x}), \quad \boldsymbol{\psi}_i \in \mathcal{S},\ \boldsymbol{\phi}_i \in \mathcal{F}. \tag{29b}$$

A parameterized P.D.E that admits a separable representation $\boldsymbol{V}(\boldsymbol{x},t;\boldsymbol{\psi})$ of order r can be defined as the function

$$\boldsymbol{V}_r(\boldsymbol{x},t) = \sum_{i=0}^{r-1} \boldsymbol{\psi}_i(t)\, \boldsymbol{\phi}_i(\boldsymbol{x}), \quad \boldsymbol{\phi}_i \in \mathcal{S},\ \boldsymbol{\phi}_i \in \mathcal{F}. \tag{30}$$

These *summands over tensor products constitute the Galerkin decomposition of the viscosity solution* $\boldsymbol{V}(\boldsymbol{x},t)$. We successively solve for the most energetic and orthogonal modes $\boldsymbol{\phi}_k(\boldsymbol{x})$, $k = 1,\cdots,n$, established via the Galerkin orthogonality criteria

$$\|\boldsymbol{V} - \boldsymbol{V}_r\|_F^2 = \min_{\substack{\{\boldsymbol{\psi}_i\}_{i=1}^{r-1}\in\mathcal{S}\\ \{\boldsymbol{\phi}_i\}_{i=1}^{r-1}\in\mathcal{F}}} \|\boldsymbol{V} - \sum_{i=0}^{r-1} \boldsymbol{\psi}_i(t)\, \boldsymbol{\phi}_i(\boldsymbol{x})\|_F^2 \tag{31}$$

$$= \min_{\substack{\boldsymbol{\Psi}\in\mathcal{S}\\ \boldsymbol{\Phi}\in\mathcal{F}}} \|\boldsymbol{V} - \boldsymbol{\Psi}(t)\boldsymbol{\Phi}(\boldsymbol{x})\|_F^2 \tag{32}$$

wi th $\boldsymbol{\Psi}(t)$ and $\boldsymbol{\Phi}(\boldsymbol{x})$ are appropriately defined. The truncation at a finite order r is reasonable in situations where the Galerkin

[5]This norm will be denoted by $\|\cdot\|_F$. When we are abusing notation, we will simply write this norm or its inner product without the F subscript.

approximations are constructed from power-form continuous functions; he

Suppose that a reduced-order basis (ROB) is already known. In an iterative fashion, we construct a reduced-order model (ROM) that solves (30) and examine the sufficiency of the solution w.r.t (25). TO-DO: In the advent of an insufficient solution, the current ROM is *enriched* with new proper generalized decomposition (PGD) functions. We adopt this PGD scheme since it has been shown to reduce the computational and storage cost of similar problems in multiscale analysis and Navier-Stokes equations [36]–[40].

We now resolve the problem stated in the foregoing. Consider an environment where $\boldsymbol{V} \in \mathbb{R}^{I_0 \times I_1 \times \cdots \times I_{N-1}}$ is a high-dimensional value function for a system of multiple interacting agents, each with dynamics $\dot{\boldsymbol{x}}_0, \dot{\boldsymbol{x}}_1, \cdots \dot{\boldsymbol{x}}_n$, and whose respective state spaces span the full rank of each mode of $\boldsymbol{V}$. Since the value functions for such a system are of high order, we replace the value function $\boldsymbol{V}(\boldsymbol{x}, t)$ with its tensor representation, $\mathbb{V}(\boldsymbol{x}, t)$ (c.f. § II) so that the full problem described in Lemma 1, corresponds to the following parameterized P.D.E

$$-\frac{\partial \mathbb{V}}{\partial t}(\boldsymbol{x}, t; \boldsymbol{\psi}) = \mathbb{W}(\mathbb{V}; \boldsymbol{\psi}),\ t \in [T, 0]\,, x \in \Omega, \boldsymbol{\psi} \in \mathcal{S} \quad (33a)$$

$$\mathbb{V}(\boldsymbol{x}, T; \boldsymbol{\psi}) = g(\boldsymbol{x}; \boldsymbol{\psi}) \quad \boldsymbol{x} \in \{\bar{\Omega} \backslash \text{int } \Omega\},\ \boldsymbol{\psi} \in \mathcal{S} \quad (33b)$$

whereupon $\mathbb{V}(\boldsymbol{x}, T; \boldsymbol{\psi})$ is contained in $L^2(\mathcal{S}; \mathcal{F})$ and $\mathbb{W}(\mathbb{V}; \boldsymbol{\psi})$ is contained in the dual space $L^2(\mathcal{S}; \breve{\mathcal{F}})$ that is associated with the space $L^2(\mathcal{S}; \mathcal{F})$.

The decomposition problem is to find $\mathbb{V} \in L^2(\mathcal{S}; \mathcal{F})$ such that $\dfrac{\partial \mathbb{V}}{\partial t} \in L^2(\mathcal{S}; \breve{\mathcal{F}})$ satisfies the boundary conditions to the initial value problem (25) and

$$\left\langle \boldsymbol{\phi}, \frac{\partial \mathbb{V}}{\partial t} \right\rangle = \langle \boldsymbol{\phi}, \mathbb{W}(\mathbb{V}; \boldsymbol{\psi}) \rangle \quad \forall\, \boldsymbol{\phi} \in \mathcal{F},\ \boldsymbol{\psi} \in \mathcal{S} \quad (34)$$

in a weak sense. The decomposition of (30) can be considered a pseudo-eigenvalue problem which proves efficient for separated representations in many applications including stochastic nonlinear PDEs [36], [37] and finite element methods [39]. The state space can be split into disjoint regions where the value function is continuously differentiable in each region. TO-DO: The *singular surfaces* [14] that separate the respective disjoint value functions constitute manifolds which have discontinuous derivative properties and we follow [41, Theorem 8.2]'s manifold resolution strategy i.e. these manifolds satisfy the saddle equilibrium strategies

$$\mathbb{H}(t; \boldsymbol{x}, \boldsymbol{u}^\star, \boldsymbol{v}) \leq \mathbb{H}(t; \boldsymbol{x}, \boldsymbol{u}^\star, \boldsymbol{v}^\star) \leq \mathbb{H}(t; \boldsymbol{x}, \boldsymbol{u}, \boldsymbol{v}^\star). \quad (35)$$

TO-DO: When the value function is not continuously differentiable; or the value function becomes discontinuous, we resort to classical fractional steps in finite differencing schemes for conservation laws [42] applied on a dimension-by-dimension basis to a mesh on which a separated composition is defined [1]. We defer the treatment of *dispersal surfaces* [14] to a future work.

The singular value decomposition of $\boldsymbol{V}$ is

$$\boldsymbol{V} = \boldsymbol{\Upsilon} \boldsymbol{\Lambda} \boldsymbol{\Theta}^T, \quad (36)$$

where, $\boldsymbol{\Upsilon} \in \mathbb{C}^{n \times r}$, $\boldsymbol{\Lambda} \in \mathbb{C}^{r \times r}$, $\boldsymbol{\Theta} \in \mathbb{C}^{m \times r}$, and $r \leq m$ can be an approximate or exact rank of $\boldsymbol{V}$. The modes of the reduced basis are the columns of $\boldsymbol{\Upsilon}$ which are ideally orthonormal i.e. $\boldsymbol{\Upsilon}^\star \boldsymbol{\Upsilon} = \mathbf{I}$, just as the columns of $\boldsymbol{\Theta}$ are as well orthonormal. From (40), the best fit operator for the parameters and basis functions are

$$\boldsymbol{\Psi} = \boldsymbol{V} \boldsymbol{\Phi}^\dagger, \text{ and } \boldsymbol{\Phi} = \boldsymbol{V} \boldsymbol{\Psi}^\dagger, \quad (37)$$

where $\boldsymbol{x}^\dagger$ denotes the Moore-Penrose inverse operator. We are concerned with the leading eigen values and eigenvectors of $\boldsymbol{V}$; therefore, we project $\boldsymbol{V}$ onto the proper orthogonal decomposition (POD) modes in $\boldsymbol{\Upsilon}$ according to

$$\boldsymbol{V}_r = \boldsymbol{\Upsilon}^T \boldsymbol{V} \boldsymbol{\Upsilon}. \quad (38)$$

This reduced model is the Galerkin projection onto the semidiscrete ordinary differential equations (o.d.e.):

$$\frac{d\boldsymbol{V}_r}{dt} = \boldsymbol{\Upsilon}^T \frac{d\boldsymbol{V}}{dt} \boldsymbol{\Upsilon}. \quad (39)$$

D. Galerkin approximation of the Variational HJI Problem

We now derive the Galerkin approximation of the viscosity solution to the terminal HJI problem. Assume that a decomposition V_r of order r is already known (this could be obtained by a partial truncation of the value function as described in § IV-H) or randomly initialized. For the next order $r+1$, a new couple $(\boldsymbol{\psi}, \boldsymbol{\phi})$ is optimal if it satisfies the Galerkin orthogonal metric

$$\begin{aligned} \|\mathbb{V} - \mathbb{V}_r\|_F^2 &= \|\mathbb{V}\|_F^2 - \sigma(\phi_i(\boldsymbol{x})) \\ &\equiv \|\mathbb{V}\|_F^2 - \|\mathbb{V}^c\|_F^2, \end{aligned} \quad (40)$$

where $\sigma(\boldsymbol{\phi}_i(\boldsymbol{x}))$ denotes an eigen decomposition of $\boldsymbol{\phi}_i(\boldsymbol{x})$ and $\mathbb{V}^c$ is the *core tensor* of $\mathbb{V}$ – representing its critical mass – which can be obtained e.g. from a high order orthogonal iteration [12] or from a higher order singular value decomposition [13], [43] of $\boldsymbol{V}$ (We discuss this in § IV-H). The optimality proof of (40) is given in appendix A via (54).

TO-DO:

Theorem 1. *Let the set* $\{\psi\}_{i=0}^{r-1} \in \mathcal{S}$ *and functions* $\{\phi\}_{i=0}^{r-1} \in \mathcal{F}$ *be vectorized as*

$$\boldsymbol{\Psi}_r^T = [\psi_0, \cdots, \psi_{r-1}]\,,\ \boldsymbol{\Phi}_r = [\phi_0, \cdots, \phi_{r-1}]^T\,, \quad (41)$$

then it follows that if the quasi-optimal basis modes have been found [6]*, the optimal Galerkin approximation of the HJI variational problem is given by*

$$\frac{\partial \mathbb{V}}{\partial t} \approx \frac{\partial \mathbb{V}_r}{\partial t} = \min \left\{ 0, \max_{\boldsymbol{u} \in \mathcal{U}} \min_{\boldsymbol{v} \in \mathcal{V}} \left\langle f(t; \boldsymbol{x}, \boldsymbol{u}, \boldsymbol{v}), \boldsymbol{\Psi}_r^T \boldsymbol{\Phi}_{\boldsymbol{x}} \right\rangle \right\}. \quad (43)$$

[6]The rationale for introducing quasi-optimality is that the best rank decomposition of the value function's tensor representation to a low-order rank tensor approximation admits accuracy only to a factor of the square root of the number of modes of the best approximation [44, Theorem 6.27] i.e.

$$\|\mathbb{V} - \hat{\mathbb{V}}\| \leq \sqrt{N} \|\mathbb{V} - \hat{\mathbb{V}}_{opt}\| \leq O(n^{3/2}) \quad (42)$$

where $\mathbb{V}_{opt}$ is the best rank-$R_0 \times R_1 \times \cdots \times R_{N-1}$ approximation of $\mathbb{V}$ and $\hat{\mathbb{V}}$ can be obtained from either Algorithm 1 or 3.

TO-DO: Work with matrices here and introduce the higher order decomposition after section IV-H.

The optimal Galerkin-approximation of the r.h.s of (33) gives

$$-\frac{\partial \mathbb{V}_r}{\partial t}(\boldsymbol{x}_r,t)=\min\left\{0,\max_{\boldsymbol{u}\in\mathcal{U}}\min_{\boldsymbol{v}\in\mathcal{V}}\left\langle f(t;x,\boldsymbol{u},\boldsymbol{v}),\left(\sum_{i=0}^{r-1}\psi_i\frac{\partial}{\partial \boldsymbol{x}}\phi_i\right)\right\rangle\right\} \tag{44}$$

The left hand side of (44)

So that given (41), we can rewrite (44) as

$$-\boldsymbol{\Psi}_r^T\dot{\boldsymbol{\Phi}}_r=\min\left\{0,\max_{\boldsymbol{u}\in\mathcal{U}}\min_{\boldsymbol{v}\in\mathcal{V}}\left\langle f(t;\boldsymbol{x},\boldsymbol{u},\boldsymbol{v}),\boldsymbol{\Psi}_r^T\boldsymbol{\Phi}_{\boldsymbol{x}}\right\rangle\right\}. \tag{45}$$

Remark 1. *Note that $\boldsymbol{\Phi}_{\boldsymbol{x}}$ are the spatial derivatives of $\{\boldsymbol{\phi}\}_{i=0}^{r-1}$ w.r.t $\boldsymbol{x}$. Furthermore, we choose not to cancel out the coefficients $\boldsymbol{\Psi}_r^T$ in (45) because we want to retain the characteristics of the original value function $\mathbb{V}(\boldsymbol{x},t)$ on the respective bases, $\{\boldsymbol{\psi}_i,\boldsymbol{\phi}_i\}_{i=0}^{r}$. At once, we see that if the optimal decomposition components $\{\boldsymbol{\psi}_i\}_{i=1}^{r}\triangleq\boldsymbol{\Psi}_r$ and $\{\boldsymbol{\phi}_i\}_{i=0}^{r-1}\triangleq\boldsymbol{\Phi}_r$ are known, equation (45) admits solutions on finite meshes, rendering solution of the separable viscosity problem (25) straightforward with the usual high precision and accuracy that Lax-Friedrichs schemes afford [1], [2], [11], [42].*

E. Galerkin HJI Approximation Under Separable Dynamics

Now, suppose that the dynamics $f(t;\boldsymbol{x},\boldsymbol{u},\boldsymbol{v})$ from (8) is separable into its state, control, and disturbance components in an additive manner as follows,

$$\dot{\boldsymbol{x}}=f(t;\boldsymbol{x},\boldsymbol{u},\boldsymbol{v}) \tag{46}$$

$$=f(t;\boldsymbol{x})\boldsymbol{x}(t)+f(t;\boldsymbol{u})\boldsymbol{u}(t)+f(t;\boldsymbol{v})\boldsymbol{v}(t), \tag{47}$$

where $f(t;\boldsymbol{x}),f(t;\boldsymbol{u})$, and $f(t;\boldsymbol{v})$ are the respective components of the system dynamics for the state, control law, and disturbance. This separable dynamics is typically observed for autonomous systems such as Dubins vehicles in relative coordinates, quadcopters, and many natural systems[7]. An example is a system of two Dubins cars in relative coordinates [21] under constant linear speed and whose motion on is controlled by the relative orientation of the vehicles$v$ i.e.

$$\begin{bmatrix}\dot{x}\\ \dot{y}\\ \dot{\theta}\end{bmatrix}=\begin{bmatrix}x\cos\theta\\ y\sin\theta\\ \omega\end{bmatrix},\quad \omega\in\mathcal{U} \tag{48}$$

with state $\boldsymbol{x}=(x,y,\theta)$ whose components are the positions (x,y) and heading θ.

[7]Even when the separation in (47) is not possible globally, we can consider a perturbation $\delta\boldsymbol{x}$ about the state $\boldsymbol{x}$ along a nominal trajectory $\bar{\boldsymbol{x}}$ so that the system's locally linear state is iteratively measured with respect to $\boldsymbol{x}$ as it is commonly done in linear quadratic methods. We defer the treatment of these locally linearized dynamics to a future work. For an in-depth treatment, see [5], [7], [33], [34].

Theorem 2. *If the system dynamics are separable as in (47), then the right hand side of the variational HJI problem that admits separable solutions is given by*

$$\begin{aligned}-\boldsymbol{\Psi}_r^T\dot{\boldsymbol{\Phi}}_r=\min\big\{&0,\left\langle f(t;\boldsymbol{x})\boldsymbol{x}(t),\boldsymbol{\Psi}_r^T\boldsymbol{\Phi}_{\boldsymbol{x}}\right\rangle\\&+\max_{\boldsymbol{u}\in\mathcal{U}}\left\langle f(t;\boldsymbol{u})\boldsymbol{u}(t),\boldsymbol{\Psi}_r^T\boldsymbol{\Phi}_{\boldsymbol{x}}\right\rangle\\&+\min_{\boldsymbol{v}\in\mathcal{V}}\left\langle f(t;\boldsymbol{v})\boldsymbol{v}(t),\boldsymbol{\Psi}_r^T\boldsymbol{\Phi}_{\boldsymbol{x}}\right\rangle\big\}.\end{aligned} \tag{49}$$

Proof. Putting (47) into (45), we find that

$$\begin{aligned}-\boldsymbol{\Psi}_r^T\dot{\boldsymbol{\Phi}}_r=\min\Big\{0,\max_{\boldsymbol{u}\in\mathcal{U}}\min_{\boldsymbol{v}\in\mathcal{V}}\big\langle&[f(t;\boldsymbol{x})\boldsymbol{x}(t)+f(t;\boldsymbol{u})\boldsymbol{u}(t)\\&+f(t;\boldsymbol{v})\boldsymbol{v}(t)],\boldsymbol{\Psi}_r^T\boldsymbol{\Phi}_{\boldsymbol{x}}\big\rangle\Big\},\end{aligned} \tag{50}$$

so that the term on the right hand side becomes

$$\begin{aligned}\min\Big\{0,\left\langle f(t;\boldsymbol{x})\boldsymbol{x}(t),\boldsymbol{\Psi}_r^T\boldsymbol{\Phi}_{\boldsymbol{x}}\right\rangle+\max_{\boldsymbol{u}\in\mathcal{U}}\left\langle f(t;\boldsymbol{u})\boldsymbol{u}(t),\right.\\\left.\boldsymbol{\Psi}_r^T\boldsymbol{\Phi}_{\boldsymbol{x}}\right\rangle+\min_{\boldsymbol{v}\in\mathcal{V}}\left\langle f(t;\boldsymbol{v})\boldsymbol{v}(t),\boldsymbol{\Psi}_r^T\boldsymbol{\Phi}_{\boldsymbol{x}}\right\rangle\Big\}.\end{aligned} \tag{51}$$

A fortiori we have the rhs of (34) as (51) if the dynamics admits separability of the form (47). □

The attractiveness of (2) is that the respective Hamiltonians can be parallelized on multiple cores during iterations of the decomposition and then assembled on a centralized node to accelerate computation with for example, the alternating direction method of multipliers [45]. TO-DO: This is treated and an example is given in **??**

Similar to (45), (51) can be resolved on a mesh. However, when the dynamics are separable as in the foregoing, the saddle point necessary condition i.e. (**??**) allows us to find an analytic solution. TO-DO: Future work. TO-DO: Under development. A future paper?

F. Galerkin HJI Approximation Under H-∞ Worst Disturbance Control

TO-DO: Under Development

G. PGD Decomposition Scheme

It now remains for us to establish an optimal way to compute the basis and coefficients of the optimal Galerkin decomposition in (45) and (51). TO-DO: we establish a Lemma due to [43] that allows every tensor $\mathbb{V}$ to admit a higher-order singular value decomposition. In our treatment, we resort to higher-order singular value decomposition (HOSVD) [46][8], extended to N-way tensors by [47]. This consists in decomposing it into the product of a core tensor, $\mathbb{V}^c\in\mathbb{R}^{R_0\times R_1\times\cdots\times R_n}$, $(R_n\leq I_n)$, and *unit norm*

[8]In his original work, Tucker only prescribed the decomposition of a tensor for up to 3 modes.

Algorithm 1 Value Function Decomposition

1: **function** ValuePower($\mathbb{V}, \epsilon$) ▷ Fix ϵ, convergence threshold.
2: Initialize $\{U\}_{n=0}^{n=N-1}$ ▷ $\mathbb{V}_n$ left dominant single vecs.
3: Set $\delta = +\infty$ ▷ δ: Least-squares fit quality.
4: **while** $\delta > \epsilon$ **do**
5: **for** $n = 0, \cdots, N-1$ **do**
6: $\mathbf{Q}_n \leftarrow \mathbb{V} \otimes_0 \mathbf{U}_0^T \otimes_1 \mathbf{U}_1^T \cdots \otimes_{N-1} \mathbf{U}_{N-1}^T$.
7: $\mathbf{U}_n \leftarrow \frac{\mathbf{Q}_n}{\|\mathbf{Q}_n\|_2}$.
8: **end for**
9: $\delta \leftarrow \|\mathbf{U}_n^T - \mathbf{U}_{n-1}^T\|_2$ ▷ Convergence check.
10: **end while**
11: $\mathbb{V}^c \leftarrow \mathbb{V} \otimes_0 \mathbf{U}_0^T \otimes_1 \mathbf{U}_1^T \cdots \otimes_{N-1} \mathbf{U}_{N-1}^T$.
12: **return** $\mathbb{V}^c, \{\mathbf{U}_n\}_{n=0}^{N-1}$.
13: **end function**

factor matrices, $\boldsymbol{U}_{n=0}^{N-1}$ of size $I_n \times R_n$ are of $\mathbb{V}$ (where $\mathbb{V} \in \mathbb{R}^{I_0 \times I_1 \times \cdots \times I_n}$)

$$\mathbb{V} \approx \hat{\mathbb{V}} \tag{52a}$$
$$= \mathbb{V}^c \otimes_0 \mathbf{U}_0 \otimes_1 \mathbf{U}_1 \otimes_2 \mathbf{U}_2 \cdots \otimes_{N-2} \mathbf{U}_{N-1}. \tag{52b}$$

The matrices $\mathbf{U}_0 \in \mathbb{R}^{I_0 \times R_0}$, $\mathbf{U}_1 \in \mathbb{R}^{I_1 \times R_1}, \cdots \mathbf{U}_{N-1}$ can be seen as representing the influence of the principal components of each mode of $\mathbb{V}$ on the *core tensor* $\mathbb{V}^c$. Put differently, in dynamical systems parlance, this can be seen as the influence of a subsystem agent's dynamics (on a value function subspace) on the overall value function of all interacting agents. The entries of $\mathbb{V}^c$ denotes level of interaction between the different components $\boldsymbol{U}_n$. They can be thought of as the critical mass of the system's interaction – encoding the objectives of the separate dynamical systems that share a large cyberphysical system space. The decomposition outlined in (52) can be obtained via the following minimization problem

$$\min_{\mathbb{V}^c, \mathbf{U}_0, \cdots, \mathbf{U}_{N-1}} \|\mathbb{V} - \mathbb{V}^c \otimes_0 \mathbf{U}_0 \cdots \otimes_{N-2} \mathbf{U}_{N-1}\|_2^2$$
$$\text{subject to } \mathbb{V}^c \in \mathbb{R}^{R_0 \times R_1 \cdots \times R_{n-1}}$$
$$\text{and orthonormal } \{\mathbf{U}\}_{n=0}^{N-1} \in \mathbb{R}^{I_n \times R_n}. \tag{53}$$

An efficient means for finding the factor matrices of minimization problem in 53 is a power iterations algorithm similar to DeLathauwer et. al's [43]. A compact representation of DeLathauwer et. al's power iteration algorithm for a general purpose tensor decomposition is presented in Algorithm 1. On line 2, the left dominant singular vector of $\mathbb{V}$ can be found via Tucker's "Method I" for computing the rank-$(R_0, R_1, \cdots, R_{N-1})$ decomposition and we refer readers to [46]. Otherwise, they can be randomly initialized as well.

On line 11 of Algorithm 1, using the orthonormal components of (52), we compute the *optimal core* $\mathbb{V}^c$ of $\mathbb{V}$ (we refer readers to [43] for a derivation) as

$$\mathbb{V}^c = \mathbb{V} \otimes_0 \mathbf{U}_0^T \otimes_1 \mathbf{U}_1^T \otimes_2 \mathbf{U}_2^T \cdots \otimes_{N-2} \mathbf{U}_{N-1}^T. \tag{54}$$

Substituting (54) into (52), we find that the approximation of $\mathbb{V}$ is a projection of the original value function tensor along its respective n-basis modes onto the reduced system, i.e.

$$\hat{\mathbb{V}} = \mathbb{V} \otimes_0 \mathbf{U}_0 \mathbf{U}_0^T \cdots \otimes_{N-2} \mathbf{U}_{N-1} \mathbf{U}_{N-1}^T. \tag{55}$$

Therefore, the approximation error is $\|\mathbb{V} - \hat{\mathbb{V}}\|^2 = \|\mathbb{V}\|^2 - \|\mathbb{V}^c\|^2$ (as shown in Appendix A).

In light of our Galerkin approximations and the validity of any resulting BRS or BRT approximation, we will work with a truncated decomposition of $\boldsymbol{V}$ at each step of the algorithm. Define the BRT or BRS up to a mode r as $\mathbb{L}_r\left[[T, 0], \mathcal{L}_0\right])$. These truncations correspond to the decomposed value function on various subspaces of the system. Because we keep the nonanticipative strategies of $\boldsymbol{P}$, the reachable set is still overapproximated in the larger sense, whereupon the pursuer makes decisions about $\boldsymbol{v}$ with full knowledge of $\boldsymbol{u}(\tau)$ for $\tau \in [t, t_f]$. Within this tolerance, we want to ensure A truncated decomposition up to mode-r would consist of a *partial core* $\mathbb{V}_r^c$ and its corresponding orthonormal matrices $\boldsymbol{U}_0, \cdots, \boldsymbol{U}_r$, $r \in [R]$ defined as

$$\mathbb{V}_r^c = \mathbb{V} \otimes_0 \mathbf{U}_0^T \otimes_1 \mathbf{U}_1^T \otimes_2 \mathbf{U}_2^T \cdots \otimes_{r-1} \mathbf{U}_r^T, \tag{56}$$

so that the truncated value function (up to mode r) is

$$\mathbb{V}_r = \mathbb{V}_r^c \otimes_0 \mathbf{U}_0 \otimes_1 \mathbf{U}_1 \otimes_2 \mathbf{U}_2 \cdots \otimes_{r-1} \mathbf{U}_r \tag{57a}$$
$$\equiv \mathbb{V} \otimes_0 \mathbf{U}_0 \mathbf{U}_0^T \otimes_1 \cdots \otimes_{r-1} \mathbf{U}_r \mathbf{U}_r^T,\ r \in [R] \tag{57b}$$

where (57b) is a result of putting (56) into (57a).

Now, revisiting the functions $\{\boldsymbol{\psi}\}_{i=0}^{r-1}$ and $\{\boldsymbol{\phi}\}_{i=0}^{r-1}$ in the previous two sections, a convenient way to compute the coefficients and basis functions that satisfy the Galerkin orthogonality criterium (40) is to set

$$\boldsymbol{\psi}_r = \mathbb{V} \otimes_0 \mathbf{U}_0^T \cdots \otimes_{r-1} \mathbf{U}_r^T \tag{58}$$

and

$$\boldsymbol{\phi}_r = \mathbb{V}_r^c \otimes_0 \mathbf{U}_0 \cdots \otimes_{r-1} \mathbf{U}_r, \tag{59}$$

where again, $\mathbf{U}_0, \cdots \mathbf{U}_{N-1}$ are factor matrices obtained from Algorithm 1.

Algorithm 2 describes how we compose the separable value function that satisfies (**??**). Lines 3 and 4 describe the optimal resolution of the decomposition parameters, $\{\boldsymbol{\psi}\}_{i=0}^{r-1}$, and basis functions, $\{\boldsymbol{\phi}\}_{i=0}^{r-1}$. In line 6 of the algorithm, the integral is solved using Total Variation Diminishing (TVD) Runge-Kutta scheme as described in [31, §3.5] (originally implemented in [48], which we re-implement in CuPy [49] as we leverage parallel computation). In addition, having r as an input variable into the algorithm allows us to take advantage of warm-starting schemes, typical in Reinforcement learning schemes [28] so that the algorithm need not be run in one fell-swoop. Partial BRT's and BRS's can be distributively learned on separate CPU/GPU cores, and later assembled on a centralized nodes to aid faster computation. TO-DO: To be developed. This may for example be similar to the alternating direction method of multipliers.

Once the respective backward reachable tubes are collected, we must stitch them together such that their composition satisfies the boundary condition of the initial value problem of (25). TO-DO: Lekan: Discuss the treatments of the singular and dispersal surfaces here.

In algorithm 2, the maximum number of iterations, r_{max} can be chosen in an informed way as highlighted below. First,

Algorithm 2 Iterative Scheme for Computing BRS/BRTs

function IterativeBRT($\mathbb{V}_{r-1}, r_{max}$) ▷ r_{max}: max. iter.
  while $r < r_{max}$ **do**
    Compute $\boldsymbol{\psi}_r$ from (58).
    Compute $\boldsymbol{\phi}_r$ from (59).
    Set $\mathbb{V}_r \leftarrow \mathbb{V}_{r-1} + \langle \psi_r, \phi_r \rangle_{\mathcal{F}}$ ▷ Update $\mathbb{V}_r$.
    Set $\langle \boldsymbol{\Psi}_r^T, \dot{\boldsymbol{\Phi}}_r \rangle_F \leftarrow \mathbb{V}_r$ c.f. (45) or (51)
    $\mathbb{L}_r \leftarrow \int_{\mathcal{S}} \langle \boldsymbol{\Psi}_r^T, \dot{\boldsymbol{\Phi}}_r \rangle_{\mathcal{F}} d\boldsymbol{x}$. ▷ Partial BRS(T), $\mathbb{L}_r$
    $r = r + 1$. ▷ Advance the decomposition.
  end while
  return $\{\mathbb{L}\}_{r=0}^{r_{max}-1}$
end function

we restate the following theorem that allows us to provide a bound on the projection error.

Theorem 3. *[Vannieuwenhoven, Vandebril, and Meerbergen] [13, Th. 5.1]. Suppose $\mathbb{V}$ is a tensor of size $I_0 \times I_1 \times \cdots \times I_{N-1}$, approximated by $\hat{\mathbb{V}}$ as in (55), the approximation error of (40) is*

$$\|\mathbb{V} - \hat{\mathbb{V}}\|_F^2 = \|\pi_0 \mathbb{V}\|_F^2 + \|\pi_1 \tilde{\mathbb{V}}_0\|_F^2 + \cdots + \|\pi_{N-1} \tilde{\mathbb{V}}_{N-2}\|_F^2. \tag{60}$$

where $\tilde{\mathbb{V}}_N$ is the partial core along mode N.

Furthermore, the approximation error is bounded by

$$\|\mathbb{V} - \hat{\mathbb{V}}\|_F^2 \leq \sum_{n=0}^{N-1} \|\pi_n \mathbb{V}\|_F^2. \tag{61}$$

Equation (61) allows us to choose an approximation error that informs us about the level of information we want preserved on the decomposed $\mathbb{V}$. Therefore, to find a decomposition $\hat{\mathbb{V}}$ of $\mathbb{V}$ whose relative decomposition error is no greater than a certain $\epsilon > 0$, we first unfold the tensor along one of its modes, compute the Gram matrix and then carry out an eigen decomposition:

$$\mathbf{G} \equiv \mathbb{V}_{(n)} \mathbb{V}_{(n)}^T = \mathbf{V} \boldsymbol{\Lambda} \mathbf{V}^T, \tag{62}$$

where $\boldsymbol{\Lambda} = \text{diag}\left(\{\lambda_1, \lambda_2, \cdots, \lambda_{I_n}\}\right)$, and $\lambda_1 \geq \lambda_2 \geq \cdots > \lambda_{I_n} \geq 0$, and $\mathbf{V}$ contains the corresponding eigenvectors. Therefore, we can choose the orthonormal matrix $\mathbf{U}_n$ and the best rank R_{n-1} tensor at mode $n-1$ as

$$\mathbf{U}_n = \mathbf{V}\,[:, 0 : R_{n-1}] \tag{63}$$

where

$$R_n = \min_{R \in [I_n]} R$$
$$\text{subject to} \sum_{i=R+1}^{I_n} \lambda_i \leq \epsilon^2 \|\mathbb{V}\|^2 / N. \tag{64}$$

Equation prescribes an informed way to choose the best rank R_r, $r \in [0, n-1]$ that satisfies the error bound in (61). An efficient way of implementing (64) is to take the cummulative sum of the diagonal terms λ_i in (62) and return the index where this is at least equal to the right hand side of (64)

$$\|\mathbb{V} \otimes_n \left(\mathbf{I} - \mathbf{U}_n \mathbf{U}_n^T\right)\|_F^2 \leq \epsilon^2 \frac{\|\mathbb{V}\|_F^2}{N}. \tag{65}$$

Algorithm 3 Incrementally Truncated Value Function [50].

function TruncatedValue($\mathbb{V}$, ϵ) ▷ ϵ: Desired accuracy.
  $\mathbb{P} \leftarrow \mathbb{V}$ ▷ $\mathbb{P}$: c.f. (3).
  for $n = 0, 1, \cdots, N-1$ **do**
    $\mathbf{G} \leftarrow \mathbb{P}_{(n)} \mathbb{P}_{(n)}^T$ ▷ $\mathbf{G}$: Gram matrix.
    $(\boldsymbol{\Lambda}, \mathbf{W}) \leftarrow \text{eig}\,(\mathbf{G})$ ▷ eig: Eigen Decomposition.
    $R_n \leftarrow \min R \in [I_n] \,|\, \sum_{i=R+1}^{I_n} \lambda_i \leq \epsilon^2 \|\mathbb{V}\|_F^2 / N$
    $\mathbf{U}_n \leftarrow \mathbf{W}\,[:, 0 : R_{n-1}]$ ▷ Orthonormal $\mathbf{U}_n$
    $\mathbb{P} \leftarrow \mathbf{G} \otimes_n \mathbf{U}_n^T$ ▷ Update partial core.
  end for
  $\mathbb{V}^c \leftarrow \mathbb{P}$ ▷ $\mathbb{V}^c$: Update core tensor.
  $\mathbf{U} \leftarrow \{\mathbf{U}_0, \cdots, U_{N-1}\}$
  return $(\mathbb{V}^c, \mathbf{U})$ ▷ $\mathbb{V}^c$: Core tensor; $\{\mathbf{U}_i\}_{i=0}^{N-1}$.
end function

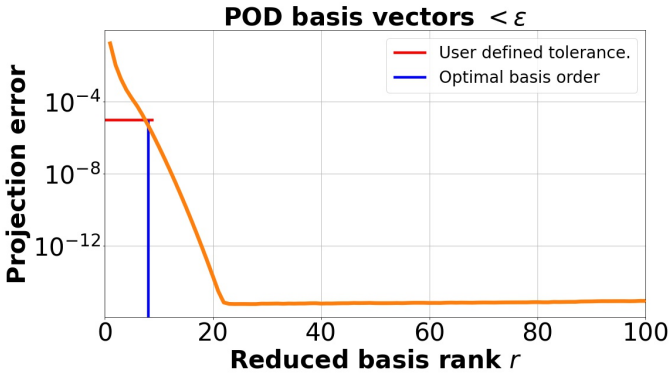

Fig. 1: Optimal basis rank given a user-defined projection error.

Whilst appealing, algorithm 2 utilizes the full value function at each step (c.f. (58)); therefore it does not easily lend itself to large-scale problems. In what follows, we propose an incrementally-constructed value function whereupon we work with the *partial cores* of $\boldsymbol{V}$ at each step of the PGD iteration. In essence, we construct the next factor matrix based on the previously computed value core.

H. Informed Incremental Value Function Decompositions

Next, we will leverage the sequentially-truncated high-order SVD of [13] to device an iteratively refined decomposition scheme onto which we will project the high-order value function. Working with partial cores, at step n, we generate the next factor matrix based on $\hat{\mathbb{V}}_{n-1}$. In particular, if the conditions of Theorem 3 hold, then

$$\|\mathbb{V} - \hat{\mathbb{V}}\|_F^2 = \|\mathbb{V} \otimes_0 \left(\mathbf{I} - \mathbf{U}_0 \mathbf{U}_0^T\right)\|_F^2 + \|\tilde{\mathbb{G}}_0 \otimes_1 \left(\mathbf{I} - \mathbf{U}_1 \mathbf{U}_1^T\right)\|_F^2 \cdots + \|\tilde{\mathbb{G}}_{N-2} \otimes_{N-1} \left(\mathbf{I} - \mathbf{U}_{N-1} \mathbf{U}_{N-1}^T\right)\|_F^2. \tag{66}$$

For convenience, we reproduce algorithm I of [13] in Algorithm 3.

V. Results and Discussion.

We now provide results and analysis of the proposed numerical algorithm on benchmark control problems.

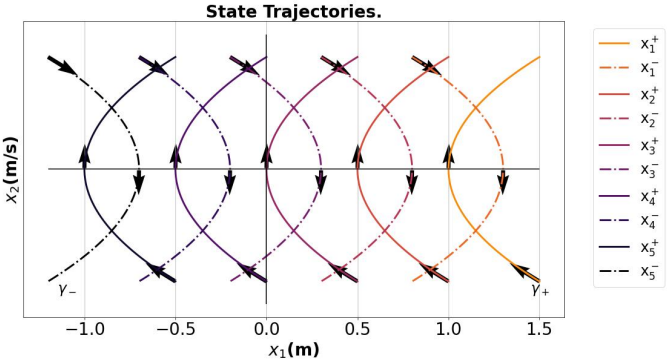

Fig. 2: State trajectories of the double integral plant. The solid curves are trajectories generated for $\boldsymbol{u} = +1$ while the dashed curves are trajectories for $\boldsymbol{u} = -1$.

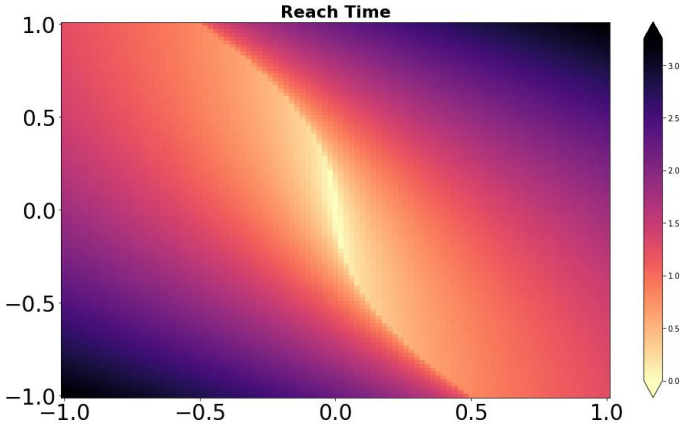

Fig. 3: Analytical time to reach the origin on the state grid, $(\mathbb{R} \times \mathbb{R})$; the switching curve corresponds to the bright orange coloration for states on $(0, 0)$.

A. Time Optimal Control of the Double Integrator

Here, we analyze our proposal on a time-optimal control problem. Specifically, we consider the double integral plant which has the following second-order dynamics

$$\ddot{\boldsymbol{x}}(t) = \boldsymbol{u}(t). \tag{67}$$

This admits bounded control signals $\mid \boldsymbol{u}(t) \mid \leq 1$ for all t. After a change of variables,we have the following system of first-order differential equations

$$\dot{\boldsymbol{x}}_1(t) = \boldsymbol{x}_2(t), \quad \dot{\boldsymbol{x}}_2(t) = \boldsymbol{u}(t), \quad \mid \boldsymbol{u}(t) \mid \leq 1.$$

The *reachability problem is to address the possibility of reaching all points in the state space in a* ***transient*** *manner*. Therefore, we set the running cost to zero, so that the Hamiltonian is $H = p_1\dot{\boldsymbol{x}}_1 + p_2\dot{\boldsymbol{x}}_2$. The necessary optimality condition stipulates that the minimizing control law is $\boldsymbol{u}(t) = -\text{ sign }(p_2(t))$. On a finite time interval, say, $t \in [t_0, t_f]$, the time-optimal $\boldsymbol{u}(t)$ is a constant k so that for initial conditions $\boldsymbol{x}_1(t_0) = \boldsymbol{\xi}_1$ and $\boldsymbol{x}_2(t_0) = \boldsymbol{\xi}_2$, it can be verified that the state trajectories obey the relation

$$\boldsymbol{x}_1(t) = \boldsymbol{\xi}_1 + \frac{1}{2}k\left(\boldsymbol{x}_2^2 - \boldsymbol{\xi}_2^2\right), \text{ where, } t = k\left(\boldsymbol{x}_2(t) - \boldsymbol{\xi}_2\right). \tag{68}$$

The trajectories traced out over a finite time horizon $t = [-1, 1]$ on a state space and under the control laws $\boldsymbol{u}(t) = \pm 1$ is depicted in Fig. 2. The curves with arrows that point upwards denote trajectories under the control law $\boldsymbol{u} = +1$; call these trajectories $\boldsymbol{\gamma}_+$; while the trajectories with dashed curves and downward pointing arrows were executed under $\boldsymbol{u} = -1$; call these trajectories $\boldsymbol{\gamma}_-$. The time to go from any point on any of the intersections to the origin on the state trajectories of Fig. 2 is our approximation problem. This minimum time admits an analytical solution [51] given by

$$t^\star(\boldsymbol{x}_1, \boldsymbol{x}_2) = \begin{cases} \boldsymbol{x}_2 + \sqrt{4\boldsymbol{x}_1 + 2\boldsymbol{x}_2^2} & \text{if } \boldsymbol{x}_1 > \frac{1}{2}\boldsymbol{x}_2|\boldsymbol{x}_2| \\ -\boldsymbol{x}_2 + \sqrt{-4\boldsymbol{x}_1 + 2\boldsymbol{x}_2^2} & \text{if } \boldsymbol{x}_1 < -\frac{1}{2}\boldsymbol{x}_2|\boldsymbol{x}_2| \\ |\boldsymbol{x}_2| & \text{if } \boldsymbol{x}_1 = \frac{1}{2}\boldsymbol{x}_2|\boldsymbol{x}_2|. \end{cases} \tag{69}$$

Let us define R_+ as the portions of the state space above the curve $\boldsymbol{\gamma}$ and R_- as the portions of the state space below the curve $\boldsymbol{\gamma}$. The confluence of the locus of points on $\boldsymbol{\gamma}_+$ and $\boldsymbol{\gamma}_-$ is the switching curve, depicted on the left inset of Fig. 3, and given as

$$\boldsymbol{\gamma} \triangleq \boldsymbol{\gamma}_+ \cup \boldsymbol{\gamma}_- = \left\{(\boldsymbol{x}_1, \boldsymbol{x}_2) : \boldsymbol{x}_1 = \frac{1}{2}\boldsymbol{x}_2 \mid \boldsymbol{x}_2 \mid\right\}. \tag{70}$$

We now state the **time-optimal control problem**: *The control problem is to find the control law that forces* (68) *to the origin* $(0, 0)$ *in the* ***shortest possible time***. The time-optimal control law, $\boldsymbol{u}^\star$, that solves this problem is unique and is

$$\begin{aligned} \boldsymbol{u}^\star &= \boldsymbol{u}^\star(\boldsymbol{x}_1, \boldsymbol{x}_2) = +1 \quad \forall\, (\boldsymbol{x}_1, \boldsymbol{x}_2) \in \boldsymbol{\gamma}_+ \cup \mathbb{R}_+ \\ \boldsymbol{u}^\star &= \boldsymbol{u}^\star(\boldsymbol{x}_1, \boldsymbol{x}_2) = -1 \quad \forall\, (\boldsymbol{x}_1, \boldsymbol{x}_2) \in \boldsymbol{\gamma}_- \cup \mathbb{R}_- \\ \boldsymbol{u}^\star &= -\text{sgn}\,\{\boldsymbol{x}_2\} \quad \forall\, (\boldsymbol{x}_1, \boldsymbol{x}_2) \in \boldsymbol{\gamma}. \end{aligned} \tag{71}$$

The minimum cost for the problem at hand is the minimum time for states $(\boldsymbol{x}_1, \boldsymbol{x}_2)$ to reach the origin $(0, 0)$, defined as

$$V^\star(\boldsymbol{x}, t) = t^\star(\boldsymbol{x}_1, \boldsymbol{x}_2) \tag{72}$$

with the associated terminal value

$$-\frac{\partial \boldsymbol{V}^\star(\boldsymbol{x}, t)}{\partial t} = \boldsymbol{H}\left(t, \boldsymbol{x}, \frac{\partial \boldsymbol{V}^\star(\boldsymbol{x}, t)}{\partial t}, \boldsymbol{u}\right)\Big|_{\substack{\boldsymbol{x}=\boldsymbol{x}^\star \\ \boldsymbol{u}=\boldsymbol{u}^\star}} \tag{73}$$

where

$$\boldsymbol{H}(t; \boldsymbol{x}, \boldsymbol{u}, p_1, p_2) = \boldsymbol{x}_2(t)p_1(t) + \boldsymbol{u}(t)p_2(t) \tag{74}$$

and

$$p_1 = \frac{\partial t^\star}{\partial \boldsymbol{x}_1}, \; p_2 = \frac{\partial t^\star}{\partial \boldsymbol{x}_2} \tag{75}$$

so that the HJ equation is

$$\begin{aligned} &\frac{\partial t^\star}{\partial t} + \boldsymbol{x}_2\frac{\partial t^\star}{\partial \boldsymbol{x}_1} - \frac{\partial t^\star}{\partial \boldsymbol{x}_2} = 0 && \text{if } \boldsymbol{x}_1 > -\frac{1}{2}\boldsymbol{x}_2|\boldsymbol{x}_2| \\ &\frac{\partial t^\star}{\partial t} + \boldsymbol{x}_2\frac{\partial t^\star}{\partial \boldsymbol{x}_1} + \frac{\partial t^\star}{\partial \boldsymbol{x}_2} = 0 && \text{if } \boldsymbol{x}_1 < -\frac{1}{2}\boldsymbol{x}_2|\boldsymbol{x}_2| \\ &\frac{\partial t^\star}{\partial t} + \boldsymbol{x}_2\frac{\partial t^\star}{\partial \boldsymbol{x}_1} - \text{sgn}\{\boldsymbol{x}_2\}\frac{\partial t^\star}{\partial \boldsymbol{x}_2} = 0 && \text{if } \boldsymbol{x}_1 = -\frac{1}{2}\boldsymbol{x}_2|\boldsymbol{x}_2|. \end{aligned} \tag{76}$$

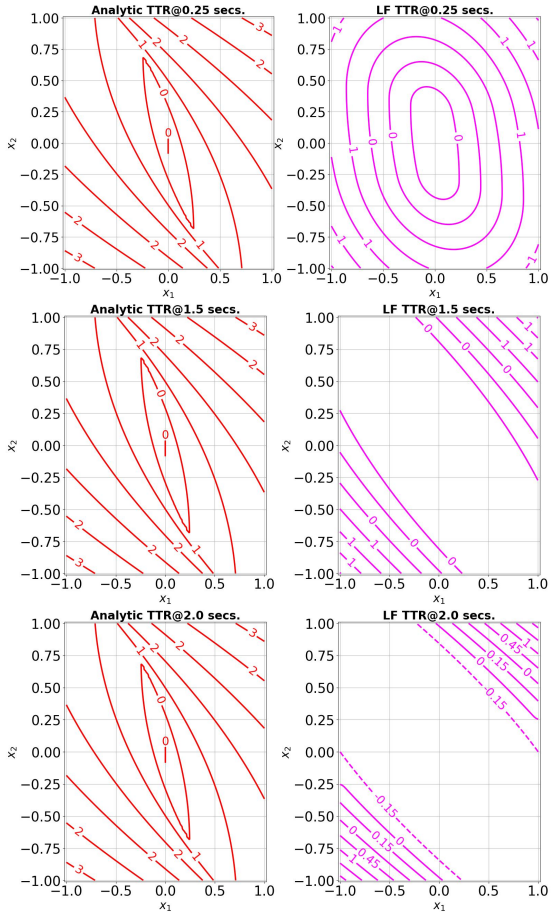

Fig. 4: Time to reach the origin at different integration steps. Left: Analytic Time to Reach the Origin. Right: Lax-Friedrichs Approximation to Time to Reach the Origin.

We compare our approximated terminal value solution using our proposal against (i) the numerical solution found via level sets methods [31] and (ii) the analytical solution of the *time to reach (TTR) the origin* problem.

A point $(\boldsymbol{x}_1, \boldsymbol{x}_2)$ on the state grid belongs to the set of states $S(t^\star)$ from which it can be forced to the origin $(0, 0)$ in the same minimum time $t^\star$. We call the set $S(t^\star)$ the minimum isochrone[9]. The level sets of (76) correspond to the *isochrones* of the system as illustrated in Fig. 4. From the results shown in Fig. 4, we see that the the approximation to the isochrones by a Lax-Fridrichs scheme (right insets in the figure) are very similar. The expansion in the sets is because we overapproximate the reachable sets at each step of the integration scheme.

B. Dubins Car Dynamics in Absolute coordinates

- All vehicles have identical dynamics
- anisotropy is reinforced by having one player being a pursuer in a local group and all other agents being evaders
- It is assumed that the roles of P and E do not change during the game, so that, when capture can occur, a necessary condition to be satisfied by the saddle-point controls of the players is the Hamiltonian (which can be derived as in Ref. 1) [21]
- controls are normalized turn rates of P and all other E's
- we turn off the capture parameter by ensuring players' speeds and maximum turn radius are equal in a flock
- to do this, make initial velocities parallel so that the equations of relative motion mean that the Evaders can maintain the initial separation forever by simply duplicating the strategy of the P. The barrier of a local flock is thus closed, so that the game of kind is ensued with finding the determination of the closed surface.

  –
- see solution to the homicidal chauffeur game in 9.1 of Isaacs

[9]These are the isochrones of the system – akin to the isochrone map used in geography, hydrology and transportation planning for depicting areas of equal travel time to a goal state.

VI. Discussions

TO-DO: Relation with Game Theory
TO-DO: Relation with Reachability analysis

VII. Conclusion.

Appendix

Appendix A
Value Function's ROM Projection Error.

The projection error between the original value function $\mathbb{V}$ and its reduced basis $\hat{\mathbb{V}}$ is

$$\begin{aligned}\|\mathbb{V} - \hat{\mathbb{V}}\|_F^2 &= \|\mathbb{V} - \mathbb{V}^c \otimes_0 \mathbf{U}_0 \cdots \otimes_{N-1} \mathbf{U}_{N-1}\|_F^2 \\ &= \|\mathbb{V}\|_F^2 - 2\langle \mathbb{V}, \mathbb{V}^c \otimes_0 \mathbf{U}_0 \cdots \otimes_{N-1} \mathbf{U}_{N-1}\rangle + \\ &\quad \|\mathbb{V}^c \otimes_0 \mathbf{U}_0 \cdots \otimes_{N-1} \mathbf{U}_{N-1}\|_F^2 \qquad (77) \\ &= \|\mathbb{V}\|_F^2 - 2\underbrace{\langle \mathbb{V} \otimes_0 \mathbf{U}_0^T \cdots \otimes_{N-1} \mathbf{U}_{N-1}^T, \mathbb{V}^c\rangle}_{\langle \mathbb{V}^c, \mathbb{V}^c\rangle} + \|\mathbb{V}^c\|_F^2\end{aligned}$$

$$\text{or } \|\mathbb{V} - \hat{\mathbb{V}}\|_F^2 = \|\mathbb{V}\|_F^2 - \|\mathbb{V}^c\|_F^2. \qquad (78)$$

References

[1] S. Osher and C.-W. Shu, "High-Order Essentially Nonoscillatory Schemes for Hamilton-Jacobi Equations," *SIAM Journal of Numerical Analysis*, vol. 28, no. 4, pp. 907–922, 1991. 1, 5, 7, 8

[2] M. G. Crandall and A. Majda, "Monotone Difference Approximations For Scalar Conservation Laws," *Mathematics of Computation*, vol. 34, no. 149, pp. 1–21, 1980. 1, 3, 8

[3] L. Evans and P. E. Souganidis, "Differential Games And Representation Formulas For Solutions Of Hamilton-Jacobi-Isaacs Equations," *Indiana Univ. Math. J*, vol. 33, no. 5, pp. 773–797, 1984. 1, 3, 5

[4] R. Bellman, *Dynamic programming*. Princeton University Press, 1957. 1, 4

[5] D. H. Jacobson, "New second-order and first-order algorithms for determining optimal control: A differential dynamic programming approach," *Journal of Optimization Theory and Applications*, vol. 2, no. 6, pp. 411–440, 1968. 1, 8

[6] D. H. Jacobson and D. Q. Mayne, *Differential Dynamic Programming*. American Elsevier Publishing Company, Inc., New York, NY, 1970. 1, 6

[7] W. Denham, "Book Reviews: Differential Dynamic Programming," *Review of Social Economy*, vol. 36, no. 2, pp. 228–229, 1978. 1, 8

[8] W. Li and E. Todorov, "Iterative linear quadratic regulator design for nonlinear biological movement systems." in *ICINCO (1)*. Citeseer, 2004, pp. 222–229. 1

[9] M. G. Crandall and P.-L. Lions, "Viscosity solutions of hamilton-jacobi equations," *Transactions of the American mathematical society*, vol. 277, no. 1, pp. 1–42, 1983. 1, 3, 4, 5

[10] I. Mitchell, "A Robust Controlled Backward Reach Tube with (Almost) Analytic Solution for Two Dubins Cars," *EPiC Series in Computing*, vol. 74, pp. 242–258, 2020. 1, 3

[11] M. G. Crandall, L. C. Evans, and P. L. Lions, "Some Properties of Viscosity Solutions of Hamilton-Jacobi Equations," *Transactions of the American Mathematical Society*, vol. 282, no. 2, p. 487, 1984. 1, 3, 8

[12] T. G. Kolda and B. W. Bader, "Tensor Decompositions And Applications," *SIAM Review*, vol. 51, no. 3, pp. 455–500, 2009. 2, 7

[13] N. Vannieuwenhoven, R. Vandebril, and K. Meerbergen, "A New Truncation Strategy for the Higher-Order Singular Value Decomposition," *SIAM Journal on Scientific Computing*, vol. 34, no. 2, pp. A1027–A1052, 2012. 2, 7, 10

[14] R. Isaacs, "Differential games: A mathematical theory with applications to warfare and pursuit, control and optimization." *Kreiger, Huntigton, NY*, 1965. 3, 7

[15] P.-L. Lions, *Generalized solutions of Hamilton-Jacobi equations*. London Pitman, 1982, vol. 69. 3, 4

[16] L. Evans and P. E. Souganidis, "Differential games and representation formulas for solutions of Hamilton-Jacobi-Isaacs equations," *Indiana Univ. Math. J*, vol. 33, no. 5, pp. 773–797, 1984. 3

[17] J. Lygeros, "On reachability and minimum cost optimal control," *Automatica*, vol. 40, no. 6, pp. 917–927, 2004. 3

[18] S. Osher and J. A. Sethian, "Fronts propagating with curvature-dependent speed: Algorithms based on hamilton-jacobi formulations," *Journal of computational physics*, vol. 79, no. 1, pp. 12–49, 1988. 3

[19] I. M. Mitchell, A. M. Bayen, and C. J. Tomlin, "A time-dependent Hamilton-Jacobi formulation of reachable sets for continuous dynamic games," *IEEE Transactions on Automatic Control*, vol. 50, no. 7, pp. 947–957, 2005. 3, 4, 5, 6

[20] L. E. Dubins, "On curves of minimal length with a constraint on average curvature, and with prescribed initial and terminal positions and tangents," *American Journal of mathematics*, vol. 79, no. 3, pp. 497–516, 1957. 4

[21] A. Merz, "The game of two identical cars," *Journal of Optimization Theory and Applications*, vol. 9, no. 5, pp. 324–343, 1972. 4, 8, 12

[22] K. Zhou and J. C. Doyle, *Essentials of Robust Control*. Prentice hall Upper Saddle River, NJ, 1998, vol. 104. 4

[23] A. Bajcsy, S. Bansal, E. Bronstein, V. Tolani, and C. J. Tomlin, "An Efficient Reachability-based Framework for Provably Safe Autonomous Navigation in Unknown Environments," in *2019 IEEE 58th Conference on Decision and Control (CDC)*. IEEE, 2019, pp. 1758–1765. 5

[24] S. Herbert, J. J. Choi, S. Sanjeev, M. Gibson, K. Sreenath, and C. J. Tomlin, "Scalable learning of safety guarantees for autonomous systems using hamilton-jacobi reachability," *arXiv preprint arXiv:2101.05916*, 2021. 5

[25] S. Bansal and C. J. Tomlin, "DeepReach: A Deep Learning Approach to High-Dimensional Reachability." 5

[26] S. Kaynama, I. M. Mitchell, M. Oishi, and G. A. Dumont, "Scalable safety-preserving robust control synthesis for continuous-time linear systems," *IEEE Transactions on Automatic Control*, vol. 60, no. 11, pp. 3065–3070, 2015. 5

[27] J. F. Fisac, A. K. Akametalu, M. N. Zeilinger, S. Kaynama, J. Gillula, and C. J. Tomlin, "A General Safety Framework for Learning-Based Control in Uncertain Robotic Systems," *IEEE Transactions on Automatic Control*, vol. 64, no. 7, pp. 2737–2752, 2019. 5

[28] J. F. Fisac, N. F. Lugovoy, V. Rubies-Royo, S. Ghosh, and C. J. Tomlin, "Bridging hamilton-jacobi safety analysis and reinforcement learning," *Proceedings - IEEE International Conference on Robotics and Automation*, vol. 2019-May, pp. 8550–8556, 2019. 5, 9

[29] M. Chen, S. L. Herbert, M. S. Vashishtha, S. Bansal, and C. J. Tomlin, "Decomposition of Reachable Sets and Tubes for a Class of Nonlinear Systems," *IEEE Transactions on Automatic Control*, vol. 63, no. 11, pp. 3675–3688, 2018. 5

[30] S. L. Herbert, M. Chen, S. Han, S. Bansal, J. F. Fisac, and C. J. Tomlin, "Fastrack: A modular framework for fast and guaranteed safe motion planning," in *2017 IEEE 56th Annual Conference on Decision and Control (CDC)*. IEEE, 2017, pp. 1517–1522. 5

[31] S. Osher and R. Fedkiw, "Level Set Methods and Dynamic Implicit Surfaces," *Applied Mechanics Reviews*, vol. 57, no. 3, pp. B15–B15, 2004. 5, 9, 12

[32] O. Ogunmolu, N. Gans, and T. Summers, "Minimax iterative dynamic game: Application to nonlinear robot control tasks," in *2018 IEEE/RSJ International Conference on Intelligent Robots and Systems (IROS)*. IEEE, 2018, pp. 6919–6925. 6

[33] S. K. Mitter, "Successive approximation methods for the solution of optimal control problems," *Automatica*, vol. 3, no. 3-4, pp. 135–149, 1966. 6, 8

[34] S. R. McReynolds, "The successive sweep method and dynamic programming," *Journal of Mathematical Analysis and Applications*, vol. 19, no. 3, pp. 565–598, 1967. 6, 8

[35] L. Kantarovich and G. Akilov, *Functional Analysis in Normed Spaces*. Pergamon Press, 1964. 6

[36] A. Nouy and O. P. Le Maıtre, "Generalized spectral decomposition for stochastic nonlinear problems," *Journal of Computational Physics*, vol. 228, no. 1, pp. 202–235, 2009. 7

[37] P. Ladevèze, *Nonlinear computational structural mechanics: new approaches and non-incremental methods of calculation*. Springer Science & Business Media, 2012. 7

[38] F. Chinesta, P. Ladeveze, and E. Cueto, "A Short Review on Model Order Reduction based on Proper Generalized Decomposition," *Archives of Computational Methods in Engineering*, vol. 18, no. 4, pp. 395–404, 2011. 7

[39] A. Nouy, "Generalized spectral decomposition method for solving stochastic finite element equations: invariant subspace problem and dedicated algorithms," *Computer Methods in Applied Mechanics and Engineering*, vol. 197, no. 51-52, pp. 4718–4736, 2008. 7

[40] A. Nouy, "A priori model reduction through Proper Generalized Decomposition for solving time-dependent partial differential equations," *Computer Methods in Applied Mechanics and Engineering*, vol. 199, no. 23-24, pp. 1603–1626, 2010. 7

[41] T. Basar and G. J. Olsder, *Dynamic noncooperative game theory*. Siam, 1999, vol. 23. 7

[42] M. Crandall and A. Majda, "The method of fractional steps for conservation laws," *Numerische Mathematik*, vol. 34, no. 3, pp. 285–314, 1980. 7, 8

[43] L. De Lathauwer, B. De Moor, and J. Vandewalle, "A multilinear singular value decomposition," *SIAM journal on Matrix Analysis and Applications*, vol. 21, no. 4, pp. 1253–1278, 2000. 7, 8, 9

[44] W. Hackbusch, *Tensor Spaces and Numerical Tensor Calculus*. Springer-Verlag, 2012. 7

[45] S. Boyd, N. Parikh, and E. Chu, *Distributed optimization and statistical learning via the alternating direction method of multipliers*. Now Publishers Inc, 2011. 8

[46] L. R. Tucker, "Some mathematical notes on three-mode factor analysis," *Psychometrika*, vol. 31, no. 3, pp. 279–311, 1966. 8, 9

[47] A. Kapteyn, H. Neudecker, and T. Wansbeek, "An Approach to n-mode Components Analysis," *Psychometrika*, vol. 51, no. 2, pp. 269–275, 1986. 8

[48] I. M. Mitchell, "A Toolbox of Level Set Methods." *UBC Department of Computer Science Technical Report TR-2007-11*, 2007. 9

[49] R. Nishino, C. Loomis, and S. Hido, "Cupy: A numpy-compatible library for nvidia gpu calculations," *31st confernce on neural information processing systems*, vol. 151, 2017. 9

[50] G. Ballard, A. Klinvex, and T. G. Kolda, "TuckerMPI: A Parallel C++/MPI Software Package for Large-scale Data Compression via the Tucker Tensor Decomposition," *ACM Transactions on Mathematical Software*, vol. 46, no. 2, 2020. 10

[51] M. Athans and P. L. Falb, *Optimal Control: An Introduction to the Theory and its Applications*. Courier Corporation, 2013. 11